Journal of
Supply Chain Management Science

Research article

Cold Chain Resilience Across Humanitarian and Resource-Constrained Settings: A Hybrid Simulation Framework

Arpish R. Solanki [1,*]

[1] Independent Researcher, India;

*Corresponding author: arpish.sol@gmail.com

Abstract: Cold chain systems are critical for preserving vaccines and other temperature-sensitive medicines, yet in fragile, resource-constrained, and crisis-affected settings, they are frequently exposed to power instability, damaged infrastructure, and extreme environmental conditions. Existing modeling approaches often emphasize supply flows while underrepresenting the interaction of thermal, logistical, and operational stressors that shape cold-chain behavior under disruption. This study introduces a hybrid simulation framework that integrates physics-based refrigeration dynamics, power availability, logistics processes, agent-driven operations, stochastic disruptions, and temperature-dependent spoilage evaluation. The framework is applied to four illustrative contexts representing heterogeneous conditions: a conflict-affected Gaza setting, a rural conflict-affected Sudan setting, a high-altitude Nepal setting, and a post-earthquake Haiti setting. Across the modeled scenarios, clinics consistently exhibited larger temperature fluctuations than depots and warehouses, while power instability emerged as a dominant contributor to thermal risk. Intervention effects varied by context; measures targeting energy availability and infrastructure generally influenced outcomes more strongly than isolated equipment upgrades. In some cases, equipment upgrades implemented without corresponding energy reinforcement increased power demand, leading to greater downtime and temperature excursions than the baseline configuration. Overall, the results indicate that cold-chain behavior under disruption is shaped by interactions among environmental, infrastructural, and operational factors rather than by equipment performance alone. The framework enables systematic exploration of these interactions and comparative analysis of cold-chain behavior across humanitarian settings.

Keywords: Cold chain resilience; Humanitarian logistics; Hybrid simulation; Power reliability; Vaccine cold storage

Publishing history: Submitted: 29 October 2025; Revised: 21 February 2026, 7 May 2026; Accepted: 2 June 2026; Published: 23 July 2026

Cite as: Solanki, A. (2026). Cold chain resilience across humanitarian and resource-constrained settings: A hybrid simulation framework. *Journal of Supply Chain Management Science*, *7*(1-2). https://doi.org/10.59490/jscms.2026.8437

ISSN: 2451-9901
Vol. 7(1-2), 2026
DOI: 10.59490/jscms.2026.8437

1 Introduction

Cold chain systems are a critical component of global public health, ensuring the safe storage and distribution of temperature-sensitive medical products such as vaccines, insulin, and biologics (Goebel, 2024; Mirai Intex, 2024). However, cold chain integrity remains highly vulnerable in many parts of the world. Nearly one billion people rely on health facilities with no or unreliable electricity, and in sub-Saharan Africa, only around 40% of facilities have reliable power, according to the World Health Organization (WHO, 2023a, 2023b). Because most routine vaccines must be stored within a narrow temperature range of 2–8°C, disruptions to refrigeration can rapidly result in product spoilage, interrupted immunization campaigns, and wasted health resources (Bajrovic & Croyle, 2023; Centers for Disease Control and Prevention, 2024; United Nations Environment Programme, 2020).

Cold chain failures occur globally but are particularly acute in fragile, conflict-affected, and disaster-prone settings. Power outages, fuel scarcity, damaged infrastructure, and security-related delays have repeatedly led to large-scale losses of vaccines and essential medicines, including documented cases in Sudan, Yemen, Papua New Guinea, Gaza, and Haiti (Hemmeda et al., 2023, 2024; Medicine Quality Research Group, 2021; OCHA, 2023, 2025b; UNICEF, 2019). Environmental stressors such as extreme heat, humidity, and large diurnal temperature swings further exacerbate these risks by reducing thermal margins and shortening safe holdover times for refrigeration equipment. In such environments, cold chain failures rarely stem from a single cause but emerge from interacting infrastructural, environmental, and human factors (AKCP, 2021; Ayowole et al., 2025; Gligor et al., 2018).

A substantial body of research has addressed vaccine supply chains using optimization, discrete-event simulation, and agent-based modeling. Platforms such as HERMES have informed national and subnational immunization system design, while stability models have quantified vaccine potency loss under temperature excursions (Campa et al., 2021; Haidari et al., 2013a). However, many existing models represent thermal risk through fixed wastage rates or externally imposed temperature profiles, rather than as an emergent consequence of power instability, environmental exposure, logistical disruptions, and operational behavior. As a result, the ability of current modeling approaches to examine cold chain performance under realistic crisis conditions remains limited.

This limitation raises questions about how cold-chain vulnerability emerges under interacting stressors and how intervention effectiveness varies across contexts.

Accordingly, this study addresses the following research questions:

RQ1: To what extent can a hybrid simulation integrating thermal, energy, logistical, and behavioral processes reveal cold-chain vulnerability patterns that are not captured by conventional modeling approaches?

RQ2: How do technical, behavioral, and infrastructure-focused interventions perform under different stress conditions across humanitarian settings, and what does this reveal about the context-dependence of cold-chain vulnerability?

To address these research questions, this study introduces a hybrid simulation framework that integrates physics-based refrigeration dynamics, energy system variability, logistical processes, and human operational behavior within a unified modeling environment. The framework is designed to explore how cold chain systems respond to compound stressors and how different interventions perform under heterogeneous conditions, rather than focusing on a single failure mode or optimization objective. The study contributes the development of an integrated hybrid modeling framework and its demonstration in humanitarian and resource-constrained cold-chain contexts through scenario-based stress-testing experiments designed to examine system responses under diverse stress conditions.

The framework is applied to four contrasting humanitarian and resource-constrained contexts that include Gaza, rural Sudan, the Nepal Highlands, and post-earthquake Haiti. They represent distinct combinations of environmental, infrastructural, and operational stressors and allow a comparative examination of how intervention effectiveness and system behavior vary across fragile settings.

The remainder of the paper is organized as follows. Section 2 introduces the background and conceptual framing. Section 3 details the hybrid simulation framework. Section 4 presents results from the simulation experiments across the four illustrative scenarios. Section 5 discusses the implications for understanding cold-chain vulnerability and intervention effectiveness across contexts, and Section 6 concludes the study.

2 Background and Conceptual Framing

2.1 Operational Characteristics of Crisis and Fragile Settings

Compound stressors in humanitarian and crisis-affected contexts are qualitatively different from those in stable settings. Power outages in such environments are often prolonged and highly unpredictable, and routine backup options may be constrained by fuel scarcity, insecurity, or limited maintenance capacity (Human Rights Watch, 2024; Médecins Sans Frontières, 2025; UN Institute for Training and Research, 2022). For example, nationwide power failures during periods of conflict have been reported to compromise national vaccine and insulin stocks in settings such as Sudan and Yemen (Save the Children, 2023; UNICEF, 2019), illustrating how energy fragility can rapidly lead to cold-chain losses. Importantly, this vulnerability is not limited to acute crises; baseline electrification levels in many settings remain uneven, particularly outside urban centers. For example, a study by Mohammed et al. (2025) reports substantially lower electricity access in rural areas of Sudan compared with urban regions, while conflict-related damage to power assets further undermines reliable energy for health services. Such structural deficits mean that cold-chain systems in these contexts often operate close to failure even before additional shocks occur. Timely delivery and maintenance access are further hampered by damaged infrastructure, checkpoints, or insecurity that disrupt transport routes and logistics (Comes et al., 2018; OCHA, 2025a).

Routine staffing, supervision, and preventive maintenance processes are also frequently disrupted during crises, which reduces the ability to detect and correct emerging cold-chain failures (Reuters, 2025; OCHA, 2024). Environmental stressors compound these vulnerabilities. Extreme heat in arid regions and hot, humid climates can accelerate thermal excursions during outages, while large diurnal temperature swings in high-altitude settings reduce equipment holdover margins, particularly when passive cooling dominates (Ayowole et al., 2025; Ng et al., 2020). These factors combine to create compound exposure pathways that are central to understanding spoilage and service interruptions in such settings. As a result, prior programmatic and operational analyses underscore the importance of accounting for interacting energy, environmental, and logistical stressors when assessing cold-chain vulnerability (Chukwuka et al., 2024; Feyisa et al., 2021; Kruczkiewicz et al., 2021).

From a supply chain perspective, these conditions imply that cold-chain performance in humanitarian settings cannot be evaluated solely through throughput, inventory availability, or routing efficiency. Reliability, service continuity, and product integrity emerge from the interaction of interdependent system conditions over time. Consequently, degradation and loss are not simply external disturbances to an otherwise stable supply network, but endogenous outcomes of how the system operates under stress. These characteristics motivate a system-level framing of cold-chain dynamics under stress.

2.2 Cold Chain Resilience as an Operational System Property

Building on these operational characteristics, this study treats cold chain resilience as a multi-dimensional system property that is demonstrated by operational and thermal outcomes under stress, rather than as a single scalar indicator. This operational framing is motivated by contemporary resilience perspectives that focus on system response and recovery dynamics over time, rather than on static or composite resilience indices (Bruneau & Reinhorn, 2006; Kruk et al., 2015; Linkov et al., 2013). Specifically, resilience is operationalized through the system's ability to (i) limit thermal and inventory degradation during disruptions, (ii) sustain service continuity, (iii) recover acceptable operating conditions following disruptions, and (iv) maintain functionality across heterogeneous stressors. Table 1 maps these resilience dimensions to the operational indicators used in the analysis and reported in the Results. To operationalize this perspective, it is necessary to distinguish resilience from related system properties commonly used in cold-chain analysis.

Table 1. Mapping of resilience dimensions to operational indicators used in the analysis.

Resilience dimension	Indicator(s) used
Degradation	Temperature excursions, unsafe exposure, spoilage fraction
Service continuity	Refrigeration downtime, delivery success
Recovery	Recovery time
Functionality under stress	Cross-scenario and intervention-based comparisons

2.3 Distinguishing Performance, Reliability, and Resilience

Within this framing, it is useful to distinguish three related but distinct concepts. Performance denotes baseline outputs under nominal conditions (for example, delivery volumes or temperature compliance), often summarized by KPI point-estimates or averages (Tang, 2024). Reliability refers to component-level availability or the probability that a component (e.g., refrigerator, generator, or grid connection) performs its intended function over a specified period (SEBoK, 2025). Resilience denotes a time-dependent, system-level capacity to absorb disturbance, adapt operations, and recover functionality (commonly framed around robustness, rapidity, resourcefulness, and redundancy) (Bruneau & Reinhorn, 2006; Kruk et al., 2015). These distinctions highlight that resilience requires modeling time-dependent system interactions, which has implications for how cold-chain systems are represented analytically.

2.4 Scope and Coverage of Existing Cold Chain Models

Against this background, prior work on cold-chain analysis clusters into three complementary methodological families.

Discrete-event and optimization models (e.g., HERMES and EPI-network studies) provide tractable tools for modelling stock flows, scheduling, allocation, and capacity trade-offs, and have been applied to national and subnational vaccine-network design (De Boeck et al., 2018; Lee et al., 2016; Mueller et al., 2016) and pandemic-era distribution planning (Chen et al., 2025; Işık & Yildiz, 2023; Khalilpoor et al., 2025; Pareja Yale et al., 2020). These methods support policy comparison, cost–coverage analysis, and extensions for multimodal delivery and equity-aware routing.

Agent-based and hybrid simulations represent actor heterogeneity, coordination failures, and stochastic disruptions, making them appropriate to study siting, demand dynamics, and operational resilience in crisis contexts (Kargar et al., 2024; Kim et al., 2022; Wang & Zhang, 2019). Complementary operational and implementation frameworks (including program guidance used by agencies) provide structures for translating modeling insights into actionable indicators for program design and monitoring (Hay et al., 2025; UNICEF, n.d., 2021b; WHO, n.d., 2018).

Pharmaceutical stability and kinetic approaches (e.g., Arrhenius models, accelerated predictive stability, mean kinetic temperature) provide the mechanistic and statistical mappings that translate temperature histories into potency loss and spoilage risk; these methods are essential for assessing health-relevant impacts of thermal exposure (Clénet, 2018; Jenkins et al., 2022; Scaccia et al., 2025).

While these approaches provide valuable insights, they reflect differing assumptions about how system dynamics, thermal processes, and operational behavior are represented. From this mapping, a persistent gap has been identified. Existing frameworks do not generate temperature histories endogenously from tightly coupled energy, thermal, and operational dynamics; instead, these processes are typically represented in a partially coupled or decoupled manner. This is the regime where interaction-driven failures most often arise in crisis-affected cold chains. In practice, this fragmentation produces three recurring limitations. First, flow-oriented and optimization models often underrepresent storage conditions, holdover limits, and power fragility, while emphasizing transport cost, carbon emissions, and scheduling with simplified treatment of thermal behavior (Li et al., 2025). Second, many ABM and hybrid studies do not fully connect handling- and power-driven thermal dynamics to agent behavior at the storage-unit level, since agent-based supply chain frameworks typically model social and physical layers without embedded heat transfer physics (De Luca et al., 2022; Fan et al., 2021; Kim et al., 2022). Third, stability and degradation models are frequently applied post hoc to externally supplied temperature traces, which restricts causal inference about why exposures occur and how interventions alter their likelihood. This simplification has been noted in cold chain energy and quality analyses that treat temperature profiles as inputs rather than emergent state variables (De Boeck et al., 2018; Marchi & Zanoni, 2022).

Across these methodological traditions, most applications focus on commercial, public-sector, or national immunization planning. Research situated in humanitarian and emergency contexts, particularly with attention to cold-chain operations, represents a smaller portion of the literature. Studies on emergency vaccine delivery and humanitarian logistics typically emphasize routing, coverage, equity, and aggregate capacity planning, which reflects the prevailing decision scales and data availability in such settings (Fahrni et al., 2022; Khodaee et al., 2022).

The present study is positioned to address this gap by integrating lumped-parameter thermal models, node-level energy subsystems, inventory degradation rules, and agent-driven operational logic within a single simulation architecture, allowing mechanism-level comparison of interventions under stress.

3 Simulation Framework and Methods

3.1 Model Overview and Scope

This study uses a hybrid simulation framework that combines discrete-time agent-driven processes with physics-informed thermal and energy submodels to examine cold-chain fragility under stress.

The simulated system is represented as a temporal network of storage and transfer nodes. Each node incorporates refrigeration units, local power subsystems, inventory batches, and operational agents. System dynamics are influenced by continuous environmental variables (such as ambient temperature and solar availability) and discrete stochastic disruptions. Subsystem coupling is crucial; power availability limits refrigeration operation; refrigeration performance determines internal temperature dynamics; accumulated thermal exposure determines inventory degradation; and agent activities influence these processes over time (Figure 1).

Two research questions are addressed by the framework's structure. The analysis of mechanism-level vulnerability (RQ1) is operationalized through component definitions, process flow, and subsystem coupling (Sections 3.2–3.4), and comparative evaluation of interventions (RQ2) is supported by scenario configuration and experimental design (Section 3.5).

Calibrated forecasts, real-time control methods, and optimization procedures are not included in the model. Rather, the framework is intended as an exploratory stress-testing tool, examining relative system behavior and identifying dominant risk drivers across parameterized scenarios and controlled comparisons, rather than providing predictive or probabilistically calibrated outputs.

3.2 System Components and State Representation

The model is composed of a small set of discrete entity classes representing physical infrastructure, inventory, and operational actors. Each entity maintains a minimal internal state that is updated at fixed simulation timesteps and may trigger time-driven events or stochastic disruptions handled within the simulation loop (Section 3.3). Entity definitions, core state variables, and primary interactions are described below, while detailed behavioral logic and subsystem coupling are discussed separately.

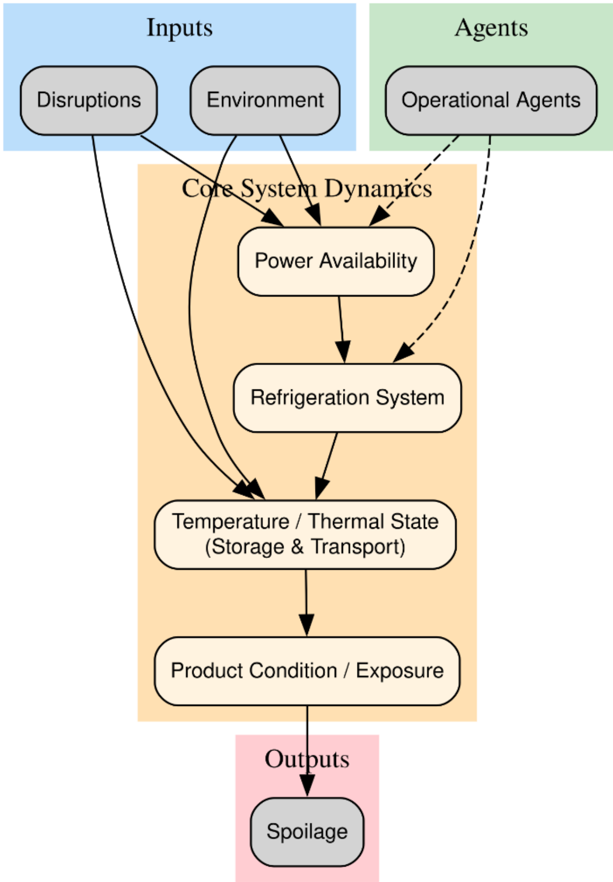

Figure 1. Conceptual system-level representation of the simulation framework, illustrating the main causal relationships between environmental drivers, power availability, refrigeration, thermal state, and spoilage outcomes. Disruptions act as external stressors, while operational agents influence system components through actions such as maintenance and handling.

3.2.1 Cold Chain Nodes (warehouses, depots, clinics)

Cold chain nodes represent locations in the logistics network where storage, transfer, and operational activities occur. Each node hosts a refrigeration unit, inventory batches, a local power system, and optional operational agents, and is characterized by a node identifier and type. Node state includes refrigerator temperature, inventory contents, and power availability as determined by its local power system. Nodes serve as origins, destinations, or transfer points for inventory movement, and their hosted components are exposed to local environmental conditions passed in at each timestep.

3.2.2 Refrigeration Units (active fridges and passive containers)

Refrigeration is represented by two related entity types: active refrigeration units located at nodes and passive transport containers. Each active unit maintains a state defined by internal temperature, effective thermal mass, insulation resistance, cooling capacity, and thermostat bounds. Cooling power is applied conditionally based on node-level energy availability, such that compressor activity is implicitly reflected in the cooling term when power is present.

Passive transport containers are modeled as non-powered insulated entities with finite latent cooling capacity, characterized by ice-pack energy reserves and melt state. Both entity types exchange heat with local ambient conditions and update their internal thermal state in response to transient disturbances. Their temperature evolution follows the governing rules specified in Section 3.7.1, with active units additionally constrained by the node-level power state defined in Section 3.7.2.

3.2.3 Power Systems (grid, battery, solar, generator)

Power systems provide electrical energy to node-level loads using a cascading supply hierarchy under resource constraints. State includes grid availability, solar output estimates, battery capacity and state of charge, and generator fuel/active status. At each timestep, available sources are used to satisfy demand and charge storage when possible; shortfalls propagate downstream to affect refrigeration operation and thermal exposure (see Section 3.4).

3.2.4 Inventory Batches (temperature-sensitive items)

Inventory batches represent discrete groups of temperature-sensitive products that move together through the cold chain. Each batch holds a list of item objects, and each item stores its safe temperature bounds, allowed unsafe duration, and assigned spoilage model, while accumulating unsafe exposure over time. During simulation steps, the hosting node or transport unit passes its internal temperature to the inventory, which records exposure for each item and evaluates spoilage using the Inventory Degradation submodel (Section 3.7.3). Batches also log transfer history and aggregate outcomes for experimental reporting (Section 3.6).

3.2.5 Operational Agents (health workers, technicians, transport handlers)

Operational agents introduce variability through routine and adaptive human actions. Agents are characterized by their role, location association, operational mode, and probabilistic behavior parameters. Their discrete actions, such as door openings, repair attempts, refuelling decisions, and transfer delays or failures, modify node, power, and refrigeration states, influencing recovery and failure outcomes. Agents are stateful actors whose modes evolve stochastically in response to recent events; behavioral logic and stress adaptation are described in Section 3.7.4.

3.2.6 Global State Representation

At each simulation timestep, the global state aggregates all entity-level states (nodes, power systems, fridges, inventories, transport units, agents), the current exogenous drivers (ambient temperature, solar availability), and any stochastic disruption flags sampled for that step. Physical process models update thermal and energy states, while the simulation loop applies event effects and agent actions to evolve interactions across subsystems over time.

3.3 Process Overview and Simulation Scheduling

The simulation advances in fixed discrete timesteps with a global, synchronous clock.

3.3.1 Event Sources

Events in the simulation originate from four main sources. Exogenous drivers include time-varying ambient temperature, solar availability, and scheduled grid-availability windows that act as external forcing. Stochastic disruptions represent unscheduled disturbances, including outages, tampering, access interruptions, and transport delays; these are sampled probabilistically each timestep and then applied to nodes and transfer events. Agent-driven actions arise from stochastic operational behavior conditioned on local state and recent disruptions. Scheduled logistics events capture planned transfer activities that occur according to predefined timelines.

3.3.2 Per-Timestep Update Order

At each simulation timestep, the framework first updates time and ambient conditions, then samples stochastic disruption events. Realized events influence agent mode transitions and modify system conditions before power availability is evaluated. Node-level power states are determined through prioritized energy fallback, which governs whether active cooling can operate. Operational actions are then applied, shaping thermal dynamics within each node.

Refrigeration and transport units subsequently update their thermal states, producing temperature histories for both stationary and in-transit inventory. These histories accumulate as item-level exposure, after which spoilage conditions are evaluated. Transfer events (departures, delays, arrivals) are executed within the same timestep, and system metrics are recorded before advancing to the next iteration. Figure 2 summarizes this within-timestep interaction flow.

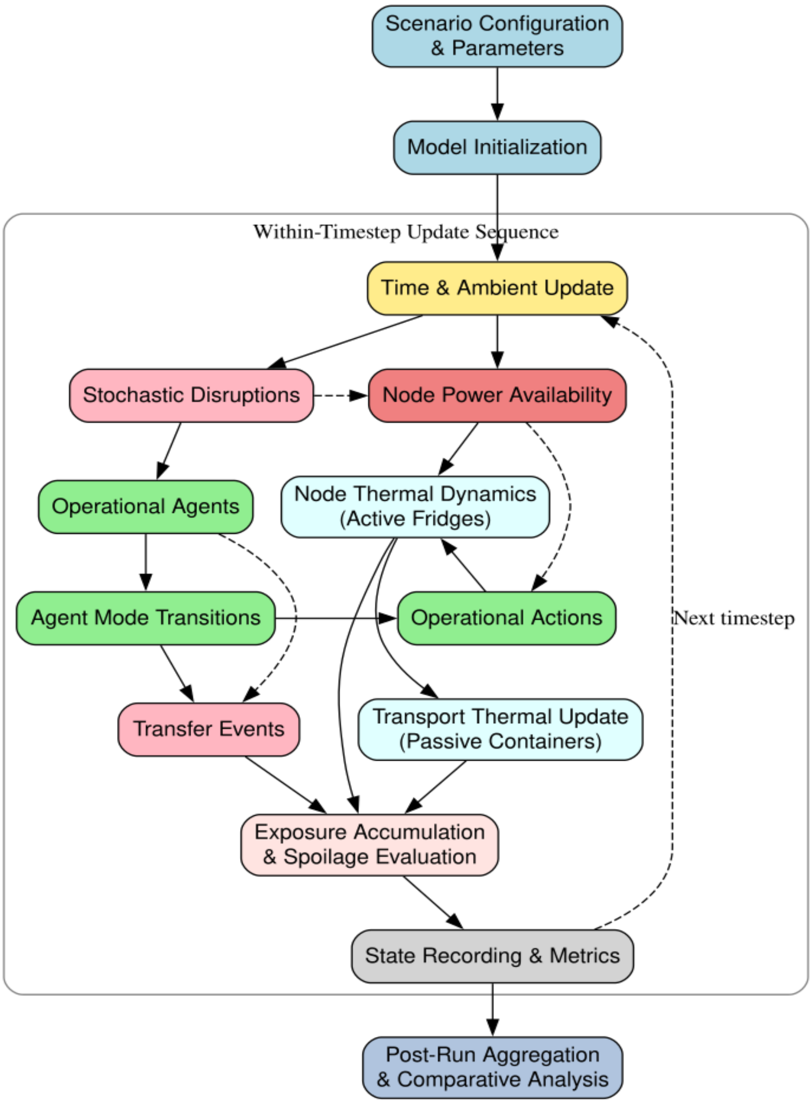

Figure 2. Per-timestep interaction flow of the hybrid cold-chain simulation, showing the update order and information dependencies between exogenous drivers, power systems, thermal dynamics, logistics agents, inventory degradation, and metrics logging.

3.4 Cross-Subsystem Interactions

The hybrid framework couples physics-based refrigeration, energy availability, logistical flows, and agent behavior to capture emergent system-level behaviors through key interaction motifs. First, a resource hierarchy introduces brittleness, where primary shortages convert into sustained cooling loss as reserves exhaust. Second, the coupling between thermal buffering and energy availability determines whether active refrigeration can operate: buffering delays excursions during transient outages but offers limited protection against prolonged deficits. Third, operational transients (agent-driven door openings or load exchanges) introduce discrete heat spikes that require concurrent cooling capacity to mitigate. Fourth, passive buffering limits in transport containers create non-linear vulnerability, with internal temperatures rapidly converging to ambient once protective reserves are depleted. Finally, delayed operational feedback from repair and refueling actions produces path dependence: finite restoration lags allow stress to accumulate into irreversible thermal loss even when mechanical failures are brief. (See Sections 3.2 and 3.7)

3.5 Scenario Configuration and Experimental Design

Experiments were organized as comparative stress tests designed to evaluate how coupled processes respond to contextual variation and to parameterized interventions. Scenario instances combined a shared hybrid simulation architecture (Sections 3.1–3.4) with scenario-specific parameter sets; because subsystem coupling produces nonlinear feedback, reported results were interpreted comparatively across scenarios and interventions rather than as calibrated point predictions.

3.5.1 Parameter classes and configuration

Parameters were grouped into three classes that capture the main drivers of cold-chain system dynamics under stress. Physical and technical parameters (e.g., refrigeration performance, battery capacity and efficiencies) were informed by manufacturer guidance and established cold-chain practice (UNICEF, 2021a; WHO, 2015). Environmental and infrastructural parameters (e.g., ambient temperature patterns, grid-availability patterns, transport-link reliability) were specified at the scenario level to approximate documented contextual conditions (Nepal Electricity Authority, 2025; OCHA, n.d.). Operational and behavioral parameters (e.g., door-opening frequency, handling practices, distributions, repair delays) were represented as bounded probabilistic ranges intended to capture plausible variability rather than calibrated forecasts (Stoddard et al., 2025; UK Health Security Agency, 2013). All parameters were normalized to the simulation timestep and were declared in structured configuration files that initialize the model; stochastic elements were sampled during runtime.

Across experiments, core modeling choices were held constant, including model architecture, timestep policy, subsystem coupling logic, agent decision structure, and output conventions. Scenario variation was introduced through targeted changes in environmental forcing, infrastructure reliability, transport and container properties, equipment quality (insulation, thermal mass, cooling sizing), and operational stressors (delays, agent availability, disruption likelihoods). All parameters were declared and ingested at initialization; access to the full configuration bundle is described in the Implementation and reproducibility note (Section 3.5.5).

3.5.2 Interventions and experiment classes

Interventions were implemented as explicit parameter modifications to baseline scenarios and were grouped into three classes: (a) infrastructure & energy measures; (b) equipment & technical upgrades; and (c) operational & behavioral measures.

Table 2. Mapping of intervention labels to system components, parameter modifications, and primary stressor mechanisms addressed. Interventions with similar underlying mechanisms are grouped under generalized labels for clarity; full parameter specifications for scenario-specific intervention variants are provided in Appendix Tables C1–C4.

Intervention	Class	System Component	Parameters Modified	Functional Effect	Stressor Addressed
Power Upgrade / Hardening	Infrastructure & Energy	Power system	Battery capacity, solar output/efficiency, generator capacity, fuel, efficiencies	Improves energy availability and resilience to outages	Power system unreliability
Resilient Grid / Shockproofing	Infrastructure & Energy	Grid infrastructure	Grid uptime, blackout probability, repair delays, disruption risks	Reduces frequency, duration, and severity of grid failures	Infrastructure / grid failure
Fridge Upgrade	Equipment & Technical	Refrigeration	Cooling capacity, insulation, thermal mass, initial temperature	Improves cooling performance and thermal stability	Ambient heat / thermal exposure
Behavior / Community Training	Operational & Behavioral	Human agents	Door behavior, misuse profile, tampering	Reduces misuse and operational heat exposure	Operational / handling variability
Robust / Improved Transport	Equipment & Technical	Logistics	Insulation, icepack mass, delay probability, routing risks	Improves transport reliability and temperature control	Access / transport constraints
Container / Mobile Units	Equipment & Technical	Transport unit	Insulation, cooling capacity, container volume	Enhances passive or mobile temperature stability	Transport-related thermal exposure
Warm Chain	Operational & Behavioral	Operational Policy	Temperature bounds, handling behavior	Relaxes strict cold constraints to reduce spoilage risk	Environmental / climatic variability

The 'Stressor Addressed' categories in Table 2 correspond to the dominant stressor classes used to characterize scenarios (Section 3.5.4) and help translate high-level stressors (e.g., power system unreliability, access constraints) into specific model-level mechanisms (e.g., grid uptime, transport delays, thermal exposure) that can be directly modified.

Interventions were evaluated individually and in combination within each scenario. Combinations were generated systematically from the primary intervention set shown in Table 2. Pairwise combinations (e.g., Power Upgrade + Fridge Upgrade, Power Upgrade + Behavior Change) and a subset of three-way combinations (up to three simultaneous interventions) were included to represent distinct policy-relevant scenarios. Due to the large number of possible configurations and the presence of cases with negligible or redundant effects, only a subset of representative combinations is reported in the Results.

Interventions were selected based on their operational feasibility within humanitarian cold chains. This approach ensures that observed outcomes are directly attributable to specific stressor–intervention interactions. Consequently, the study focuses on realistic decision spaces rather than exhaustive optimization or global searches. For experiment control, generator fuel was capped at one full run in interventions that add generator provisioning. Full parameter-change listings appear in Appendix Tables C1–C4.

3.5.3 Sampling, sensitivity, and robustness

Stochastic Sampling

Stochasticity was introduced through random disruptions, agent behavior, and event timing. Each scenario–intervention configuration was simulated across 25 independent runs with distinct random seeds. Reported outcomes were aggregated using mean values with 95% confidence intervals and complementary distributional measures.

Sensitivity Analysis

Sensitivity to parameter variation was evaluated using one-at-a-time perturbations of 13 subsystem parameters spanning power reliability, refrigeration performance, and transport conditions (e.g., blackout chances, grid uptime, battery capacity, insulation).

Each parameter was varied across −30%, −10%, baseline, +10%, and +30%, with all other parameters held constant. Simulations were repeated using the same stochastic sampling procedure. Outcomes were compared against the baseline configuration; perturbations primarily affected outcome variability rather than central tendencies, with limited shifts in median performance. No qualitative reversals in system behavior were observed.

Temporal Resolution and Robustness Checks

Sensitivity to temporal discretization was assessed using 5-minute, 10-minute, and 15-minute timestep resolutions. While finer resolutions affected the magnitude of time-dependent metrics, no qualitative changes were observed in system behavior or intervention ranking.

Additionally, a subset of representative scenario–intervention configurations was re-simulated with independent seed sets to confirm the stability of aggregated outcomes and intervention rankings, with no qualitative changes observed across runs.

3.5.4 Scenario archetypes

Four illustrative scenarios were developed to investigate cold-chain behavior under stress across diverse humanitarian contexts. These archetypes (summarized in Table 3) represented distinct combinations of environmental, infrastructural, and operational stressors selected during the experimental design.

Gaza conflict-affected setting: Focused on acute energy insecurity and security-related and access constraints in a high-temperature urban environment. It tested the system’s reliance on intermittent solar and generator fallbacks under severe grid instability.

Sudan rural conflict-affected setting: Represented extreme heat combined with fragile, low-efficiency equipment. This scenario emphasized the impact of logistical roadblocks and delayed maintenance in remote, resource-limited regions.

Nepal highlands setting: Examined cold-climate challenges where terrain and altitude dominated logistics. Unlike the conflict scenarios, the primary stressors were modeled as transport disruptions rather than power failures.

Haiti post-earthquake setting: Captured a systemic collapse where damaged infrastructure led to extreme energy insecurity (≈30% grid uptime) and logistical bottlenecks in a hot, humid tropical setting.

Parameters for these scenarios were synthesized from humanitarian literature and secondary regional reports rather than primary field observations or agency-specific datasets. This approach allowed the use of stress tests designed to examine the simulation framework across diverse crisis archetypes.

Table 3. Qualitative scenario dimensions for four illustrative archetypes. Cells use role-anchored descriptors (clinic / depot / warehouse) and relative, non-numeric terms to support cross-scenario comparison. Common constants: same spoilage kinetics, inventory types, and core refrigeration model across scenarios; only stressors and relative device specs vary. Numeric parameters and full specifications appear in a structured configuration file.

Dimension (qualitative)	Gaza (conflict-affected)	Sudan (rural, conflict-affected)	Nepal (highlands)	Haiti (post-earthquake)
Primary analytical role	Focus: security- & power-driven operational fragility. Key mechanism: access disruptions leading to power loss.	Focus: heat- & access-driven operational fragility. Key mechanism: delays under high heat.	Focus: environment-/terrain-driven thermal & access fragility. Key mechanism: altitude/terrain impacts on transport.	Focus: post-disaster systemic collapse (power, transport, logistics). Key mechanism: combined infrastructure failure.
Ambient climate	Day/night: hot days, warm nights; Humidity: low–moderate.	Day/night: very hot days, warm nights; Humidity: low–moderate.	Day/night: cool days, near-freezing nights; Humidity: low.	Day/night: hot & humid; Humidity: high.
Grid reliability (structural)	Structural reliability: low; Scheduling: rationed on-windows.	Structural reliability: moderate; Scheduling: prioritized at hubs.	Structural reliability: high (valleys); Scheduling: generally steady.	Structural reliability: very low; Scheduling: widely irregular.
Blackout pattern (temporal)	Frequency: occasional unexpected outages; Pattern: tied to rationing windows.	Frequency: frequent/intermittent outages; Pattern: hubs prioritized.	Frequency: occasional short outages; Pattern: weather/microgrid-related.	Frequency: widespread, irregular outages; Pattern: post-event damage.
Local backup provisioning	Availability: mixed — warehouses better than clinics; Fuel/logistics: constrained.	Availability: moderate — depots/warehouses better; Clinics limited.	Availability: moderate–good — batteries/gensets common at facilities.	Availability: partial — gensets/batteries present but fuel/logistics constrained.

Dimension (qualitative)	Gaza (conflict-affected)	Sudan (rural, conflict-affected)	Nepal (highlands)	Haiti (post-earthquake)
Refrigeration baseline (clinic / depot / warehouse)	Clinic: smallest units; Depot: intermediate; Warehouse: large. Insulation: moderate.	Clinic: very small, low-spec; Depot: small; Warehouse: intermediate. Insulation: low–moderate.	Clinic: small; Depot: intermediate; Warehouse: large. Insulation: good.	Clinic: small; Depot: intermediate; Warehouse: large. Insulation: moderate.
Transport / access constraints	Level: high; Typical causes: blockades, checkpoints, unpredictable delays.	Level: high; Typical causes: poor road conditions, conflict-related diversions.	Level: high (seasonal); Typical causes: landslides, monsoon impacts, terrain.	Level: high; Typical causes: road/bridge damage, debris obstruction, fuel shortages.
Security risk	Level: elevated; Nature: conflict-related disruptions.	Level: low–moderate; Nature: localized security incidents.	Level: minimal; Nature: negligible security risk.	Level: elevated; Nature: opportunistic post-event security risk.
Repair & spare-parts availability	Availability: low; Typical delays: long due to access and supply constraints.	Availability: very low; Typical delays: long and remote.	Availability: moderate; Typical delays: terrain-related shipping lags.	Availability: low; Typical delays: disrupted supply chains.
Agent handling behaviour	Handling mode: predominantly multi-use; Access regularity: highly irregular; Care level: variable.	Handling mode: predominantly multi-use; Access regularity: moderately irregular; Care level: variable.	Handling mode: careful–multiuse mix; Access regularity: largely regular; Care level: relatively high.	Handling mode: predominantly multi-use; Access regularity: mixed/unstable; Care level: mixed.
Clinic battery buffer	Buffer: moderate; Typical duration: short (partial-day).	Buffer: small; Typical duration: short.	Buffer: moderate; Typical duration: sufficient for short outages.	Buffer: moderate; Typical duration: partial-day.
Dominant stressor class	Primary stressors: power + security.	Primary stressors: heat + access.	Primary stressors: environment + terrain.	Primary stressors: power + transport + logistics.
Operational instability	Level: high; Main drivers: security-related disruptions and unreliable power supply.	Level: moderate; Main drivers: heat-induced operational strain and limited road accessibility.	Level: low; Main drivers: seasonal transport variability.	Level: very high; Main drivers: systemic infrastructure collapse.

For brevity, scenarios are referred to by geographic archetypes (e.g., “Sudan”, “Gaza”); these labels reflect context-informed, stylized representations of operational conditions rather than exhaustive regional models. One clinic in each scenario was intentionally deprived of regular delivery to reflect service inequalities commonly observed in humanitarian settings and to introduce asymmetric stress within the network. Figure 3 shows representative grid availability profiles used as scenario inputs for each archetype.

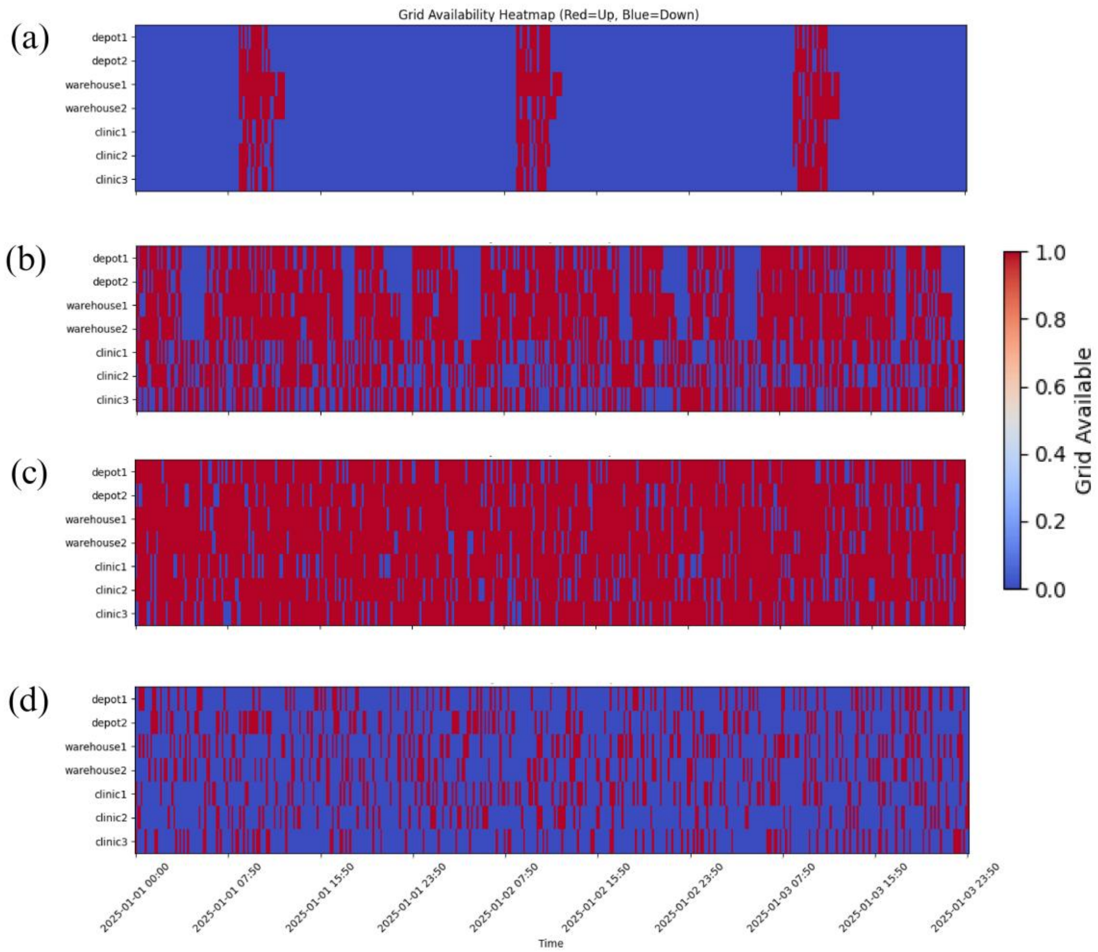

Figure 3. Representative grid availability profiles generated by the power subsystem for each scenario (a) Gaza, (b) Rural Sudan, (c) Nepal Highlands, and (d) post-earthquake Haiti. Heatmaps visualize simulated on/off-grid supply over time based on scenario-specific configuration of availability windows, outage processes, and disruption events. These profiles function as time-varying forcing inputs for downstream refrigeration and cold-chain processes. Scenario configurations differ in the severity and regularity of grid supply, with relative distinctions across warehouses, depots, and clinics encoded through their respective power system specifications.

3.5.5 Implementation and reproducibility note

All scenario definitions, parameter ranges, and intervention settings were expressed in structured configuration files ingested at initialization. The full configuration bundle, materials, and code are available in the public repositories referenced in the Data/Software Access Statement.

3.6 Output Metrics and Observed System Indicators

3.6.1 Logged Outputs

Each simulation run produced structured component-level logs that record system evolution over time. Logged variables captured thermal behavior, energy availability, inventory condition, and operational activity across storage, transport, and handling processes. Thermal and refrigeration logs included internal temperature readings for stationary and transport units. Power system logs recorded grid availability, battery state of charge, generator status and fuel levels, and the power sources selected at each timestep. Inventory logs tracked batch-level temperature exposure histories and spoilage events as determined by the assigned degradation models. Operational and logistics logs captured transport departures and arrivals, transfer events, and agent actions and mode transitions. At run completion, all raw logs were retained, with a small set of convenience aggregates computed for summary reporting; all reported results were derived from the underlying logs.

3.6.2 Summary Aggregates

Summary aggregates were computed post-simulation from the retained logs to facilitate comparison across scenarios and interventions, particularly where large-scale variation made direct inspection of raw logs impractical. Core aggregates included the occurrence and duration of temperature excursions, defined as periods during which storage or transport units exceeded safe temperature bounds while inventory was present; cumulative unsafe exposure, representing total batch-level time spent outside acceptable limits; and refrigeration downtime, measured as the duration for which active cooling was unavailable due to power loss or exhausted backup resources. Outcome-oriented aggregates included the spoilage fraction, defined as the proportion of batches flagged as spoiled by the end of the simulation horizon, and delivery outcomes, capturing successful and failed transfers across the logistics network.

3.6.3 Observational Indicators

Several quantities discussed in the analysis were observational constructs inferred from combinations of logged variables rather than directly recorded as single state values. Recovery time was operationalized as the elapsed time between the onset of a temperature excursion beyond the safe range and return to within the safe temperature range. Power-stress indicators, including outage frequency and duration as well as battery or generator exhaustion, were derived to contextualize observed thermal and inventory outcomes. Node-level vulnerability characteristics were synthesized from temperature profiles, excursion counts, cumulative exposure, and refrigeration downtime to identify relative weak points within the system, without collapsing these dimensions into a single composite score. All such indicators were used descriptively to interpret system dynamics, without being embedded as composite indices within the model structure.

3.7 Component Submodels

The simulation framework was implemented as a set of coupled, discrete-time submodels that are sequentially updated at each timestep (Section 3.3). Each submodel captures a distinct causal mechanism. All submodels were formulated as lumped-parameter representations (no spatial resolution or PDEs), chosen to capture first-order dynamics governing exposure accumulation, remain computationally tractable under stochastic repetition, and support interpretability of intervention effects.

Sections 3.2 and 3.7 are complementary. Section 3.2 lists the entity-level states used by the simulation, while Section 3.7 describes the dynamical submodels that update those states over time.

3.7.1 Thermal and refrigeration dynamics

The thermal behavior of storage units and transport containers was modeled using a single-node energy balance with equivalent thermal resistance and capacitance. Storage units and active transport containers (motorized refrigerated vehicles) share the same thermal model: internal temperature changes in response to ambient conditions, active cooling (when available), and discrete operational events. Passive transport containers (insulated cold boxes with ice packs) were modeled separately using a piecewise thermal response, ice packs provide latent heat absorption (334 kJ/kg) until depleted, after which the container warms exponentially toward ambient.

For active refrigerated units, internal temperature was advanced each timestep using a discrete energy-balance update:

$$T_{\mathrm{fr}}(t+\Delta t) = T_{\mathrm{fr}}(t) + \frac{\Delta t}{C_{\mathrm{th}}}\left[Q_{\mathrm{cond}}(t) + Q_{\mathrm{infiltration}}(t) - P_{\mathrm{cool}}(t)\right] + \Delta T_{\mathrm{door}}(t) + \Delta T_{\mathrm{items}}(t).$$

Conductive heat transfer was modeled using an equivalent thermal resistance, while infiltration was represented as a continuous air exchange term proportional to ambient–internal temperature difference. Door openings and item insertions are treated as discrete thermal impulses. A thermostat hysteresis controller controls cooling, explicitly gated by power availability. If sufficient power cannot be supplied, active cooling is turned off, and the unit warms passively. Passive cold boxes use the same conductive and infiltration terms but substitute ice pack phase change for active cooling. Full-term definitions and control logic are provided in Appendix A.

3.7.2 Power availability and switching

This submodel determines refrigeration and auxiliary load availability per node per timestep. Sources contribute sequentially to meet residual demand; unmet demand yields service interruption. Battery state and generator fuel deplete with use, with grid/solar charging subject to implicit rate limits and efficiency effects. The abstraction captures intermittency, backup depletion, and cascading supply logic as the main drivers of downtime and recovery.

3.7.3 Inventory degradation and spoilage

This submodel converts time–temperature exposure histories into item-level spoilage outcomes. Each item type was assigned a degradation model at initialization (e.g., abrupt threshold, cumulative time exceedance, thermal stress weighting, or Arrhenius kinetics). For the Arrhenius model, temperature-dependent reaction rates are computed as:

$$k(T) = A\exp\left(-\frac{E_a}{R_u(T+273.15)}\right)$$

and

$$D(t+\Delta t) = D(t) + k\big(T(t)\big), \Delta t$$

Parameter meanings and spoilage rules are given in Appendix A. Temperature exposures were logged at 10-minute intervals; spoilage status was re-evaluated after each recorded exposure. This formulation permits representation of both abrupt and progressive deterioration processes under heterogeneous temperature exposure conditions.

3.7.4 Agent-driven operational logic

This submodel introduces human and operational variability through stochastic agent-based actors (health workers, technicians, transport agents). Agents maintain discrete behavioral modes that evolve via event-driven Markov transitions, with transition probabilities biased by recent events and stress indicators. Decision-making is probabilistic and mode-dependent; agents face stochastic delays, resource constraints, and state-triggered actions. Agent actions couple to physical submodels by modifying system state (thermal disturbances, power restoration). This captures operator fatigue, imperfect adherence, and delayed recovery without requiring explicit utility functions or optimization.

3.7.5 Event and disruption processes

This submodel represents discrete disruptions (e.g., outages, theft, tampering, roadblocks) as stochastic events evaluated at each simulation timestep. Each event type is defined by a baseline probability and, when realized, alters the state of relevant system components. Some events persist for finite durations, whereas others produce instantaneous state changes.

An instability cascade mechanism, parameterized by an index in the unit interval, allows realized events to probabilistically trigger additional disruptions, representing systemic stress or compounding instability effects. Events also influence agent behavior through state-transition dynamics. This structure embeds disruptions within the broader system dynamics, allowing their effects to propagate through interconnected processes via both direct and indirect pathways.

4 Results

This section presents baseline system behavior across scenarios, followed by a comparative evaluation of interventions and their combinations. Here, baseline refers to the unmodified scenario configuration without additional interventions, as defined in the experimental design (Section 3.5).

For most selected subsystem parameters, spoilage outcomes remained stable under ±30% parameter perturbations, with median shifts generally below ±0.003 relative to the baseline configuration. Variations in refrigeration and power-related parameters exhibited the most pronounced effects, manifesting primarily as increased dispersion across stochastic runs. As shown in Figure 4, median spoilage fractions clustered tightly around the baseline value (≈ 0.074), while interquartile ranges widened under degraded conditions.

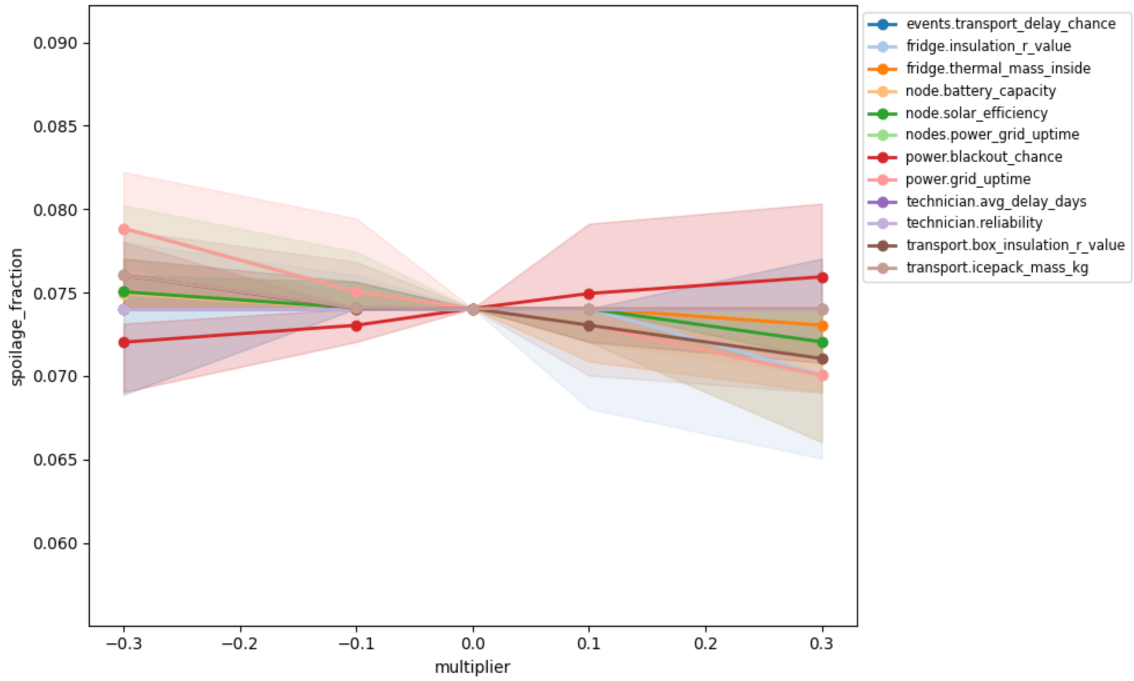

Figure 4. Spoilage fraction under ±30% perturbations of selected parameters

The simulated refrigeration systems generally maintained internal temperatures near the recommended 2–8 °C range throughout the 72-hour baseline runs in Gaza, rural Sudan, the Nepal Highlands, and post-earthquake Haiti. Depots and warehouses exhibited greater stability than clinics, with warehouses averaging 4.4–4.7 °C compared to clinic means of 5.1–5.2 °C. Clinic-level fluctuations were most evident in Gaza and Sudan, driven by high ambient peaks, while Nepal and Haiti remained closer to mid-range stability despite large day–night swings and tropical heat, respectively. Diurnal patterns were evident across all settings, with minor afternoon rises that were buffered by modeled insulation and thermal mass. In Gaza and Sudan, occasional excursions above 10 °C occurred in depots and warehouses once backup generators reached their modeled fuel cap, typically occurring at night when solar power was unavailable. Their characteristics varied by storage scale and buffering. Clinic fridges showed large excursions once cooling or passive buffers failed, while warehouse units with greater thermal mass exhibited short, transient spikes followed by rapid return to safe temperatures. Recovery following excursions was generally rapid across scenarios, typically on the order of tens of minutes. In the Sudan scenario, for example, a clinic-level excursion above 8 °C persisted for approximately 20 minutes (two simulation timesteps) before returning to within the safe range (Figure 5). Excursions were short-lived, typically occurring in conjunction with transient disruptions in energy availability. Power restoration and timely agent actions (refueling/repair) enabled the return to safe temperatures.

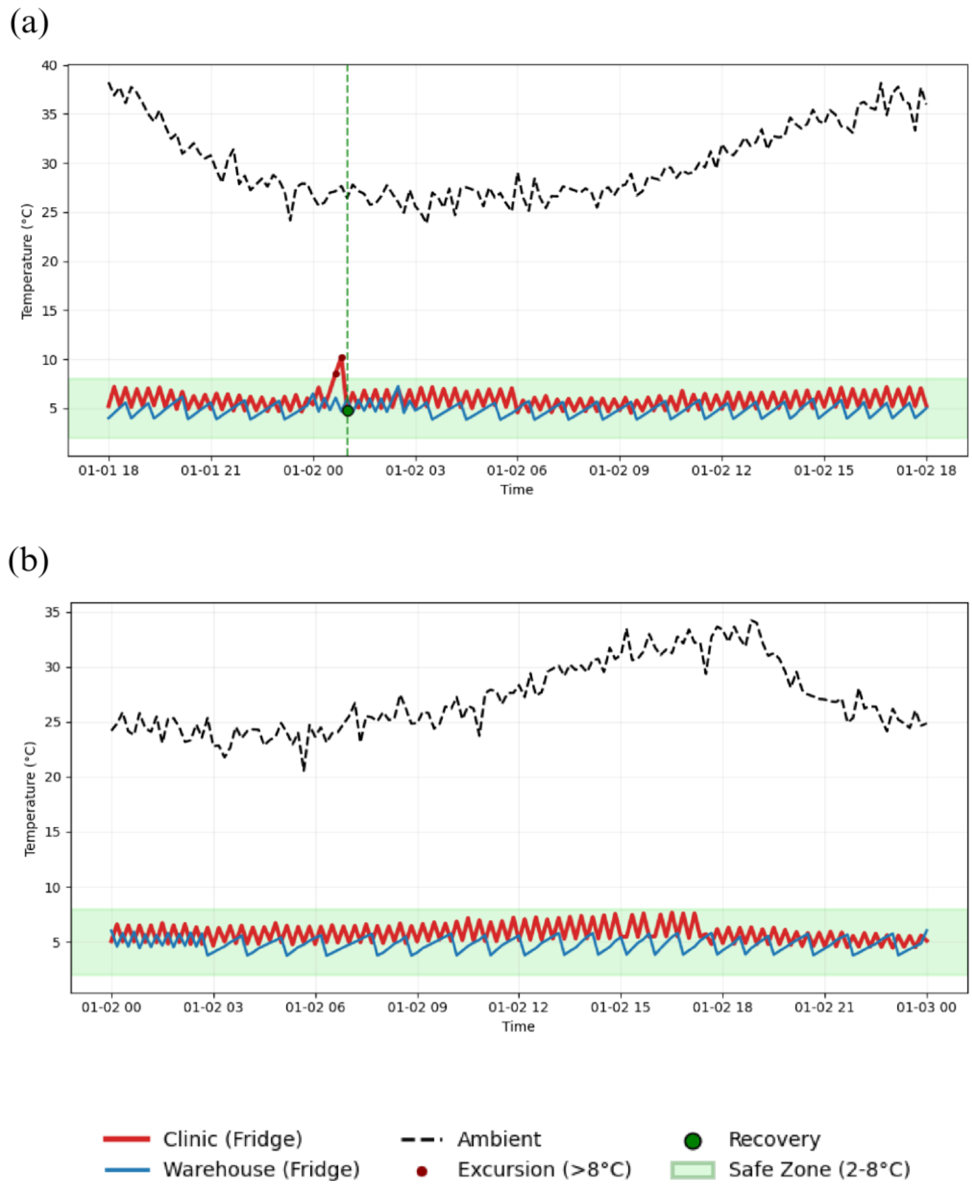

Figure 5. Representative node-level temperature dynamics under stress. (a) Sudan: a clinic unit exhibits a temperature excursion above the safe 2–8 °C range following power disruption, followed by recovery once cooling is restored. (b) Gaza: a clinic unit operates near the upper safety threshold, illustrating near-failure behavior under sustained stress without full excursion. Ambient temperature profiles (dashed lines) are shown for reference, and the shaded region indicates the safe operating range (2–8 °C). Excursion events and recovery points are highlighted.

Transport performance varied minimally. Motorbikes and vans with moderate insulation reliably maintained safe ranges in Gaza, Nepal, and Haiti, including under ambient peaks near 35 °C in high-temperature settings. By contrast, low-insulation passive units showed repeated breakdowns. In the Sudan scenario, the Bicycle1 unit peaked around 17 °C after ice depletion. Deliveries generally stabilized after ice pack replenishment (Figure 6).

(a)

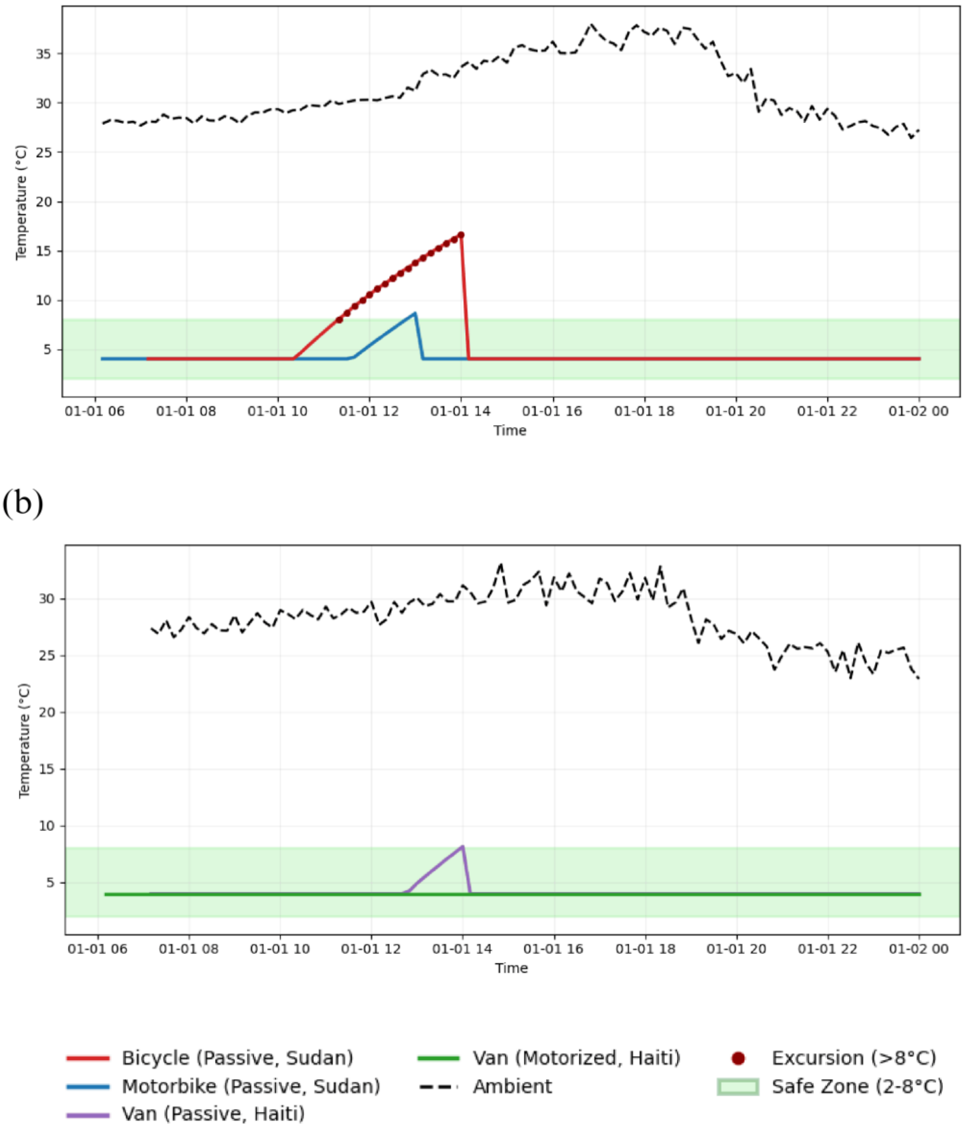

(b)

Figure 6. Representative transport unit temperature dynamics across contrasting configurations. (a) Sudan: a low-insulation bicycle transport unit exhibits a clear excursion following icepack depletion, while a motorbike unit remains near the safe threshold. (b) Haiti: comparison of two van-based systems shows improved stability under motorized refrigeration relative to a passive configuration. Ambient conditions are shown for reference (dashed lines), and the shaded region denotes the safe temperature range (2–8 °C). Excursion events are indicated.

At the logistics level, two batches were successfully delivered to clinic1 and clinic2 through their respective warehouses and depots, while clinic3 received none due to intentional design constraints. With the exception of clinic 3, all multi-step handovers were completed without failure, with exposure accumulation recorded during transfers (Figure 7).

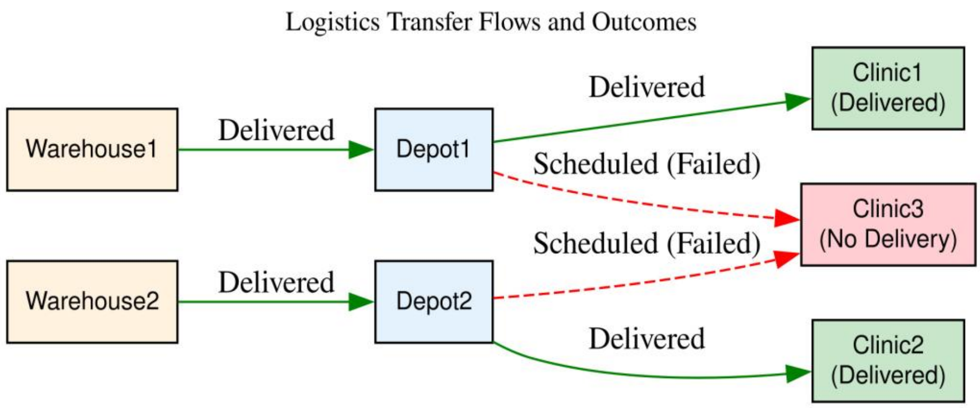

Figure 7. Transfer flows and outcomes across all scenarios. Two successful supply chains are shown from warehouses through depots to clinics, while the transfer to Clinic3 was failed because only two batches were created.

Of the ten tracked medical items, only the polio vaccine exhibited consistent spoilage under the modeled conditions. Its −20 °C storage requirement was incompatible with standard 2–8 °C refrigerators, leading to repeated spoilage across scenarios. All other items recorded minimal unsafe exposure hours, confirming that the modeled cold chain adequately preserved standard 2–8 °C products.

Grid instability was the dominant disruption, comprising 18–25% of events with stochastic outages typically lasting 30–180 minutes (mean ~100 minutes). Gaza, Sudan, and Haiti showed the highest outage frequency, while Nepal remained relatively stable, reflecting predefined grid profiles. Power shortages frequently pushed facilities into critically low battery levels, particularly at depots and clinics. Although warehouses had the largest provisioning, they too reached zero reserves when inputs faltered. These conditions reflected stress-test assumptions rather than empirical outage patterns. Other disruptions included roadblocks, delays, and low-probability events such as tampering.

Overall, baseline configurations produced low spoilage but notable variation in temperature excursions and downtime. In Gaza, the baseline averaged 27 excursions and 30 downtime hours per node; only Resilient Grid and Power Upgrade interventions meaningfully improved outcomes, nearly halving both metrics when implemented in tandem. In Sudan, the baseline logged 12 excursions and over 22 hours of downtime; Power Upgrade was the only consistently effective intervention, reducing downtime. The Fridge Upgrade alone worsened outcomes relative to baseline, and when combined with it, the Transport Upgrade also failed to produce improvement. In Nepal, baseline conditions were stable (9 hours of downtime), and most interventions yielded no measurable gains. In post-earthquake Haiti, grid conditions remained highly unstable (16 excursions, 25 downtime hours); only Power Hardening and Infrastructure Shockproofing provided significant improvement, while other interventions showed little benefit (Figures 8 and 9).

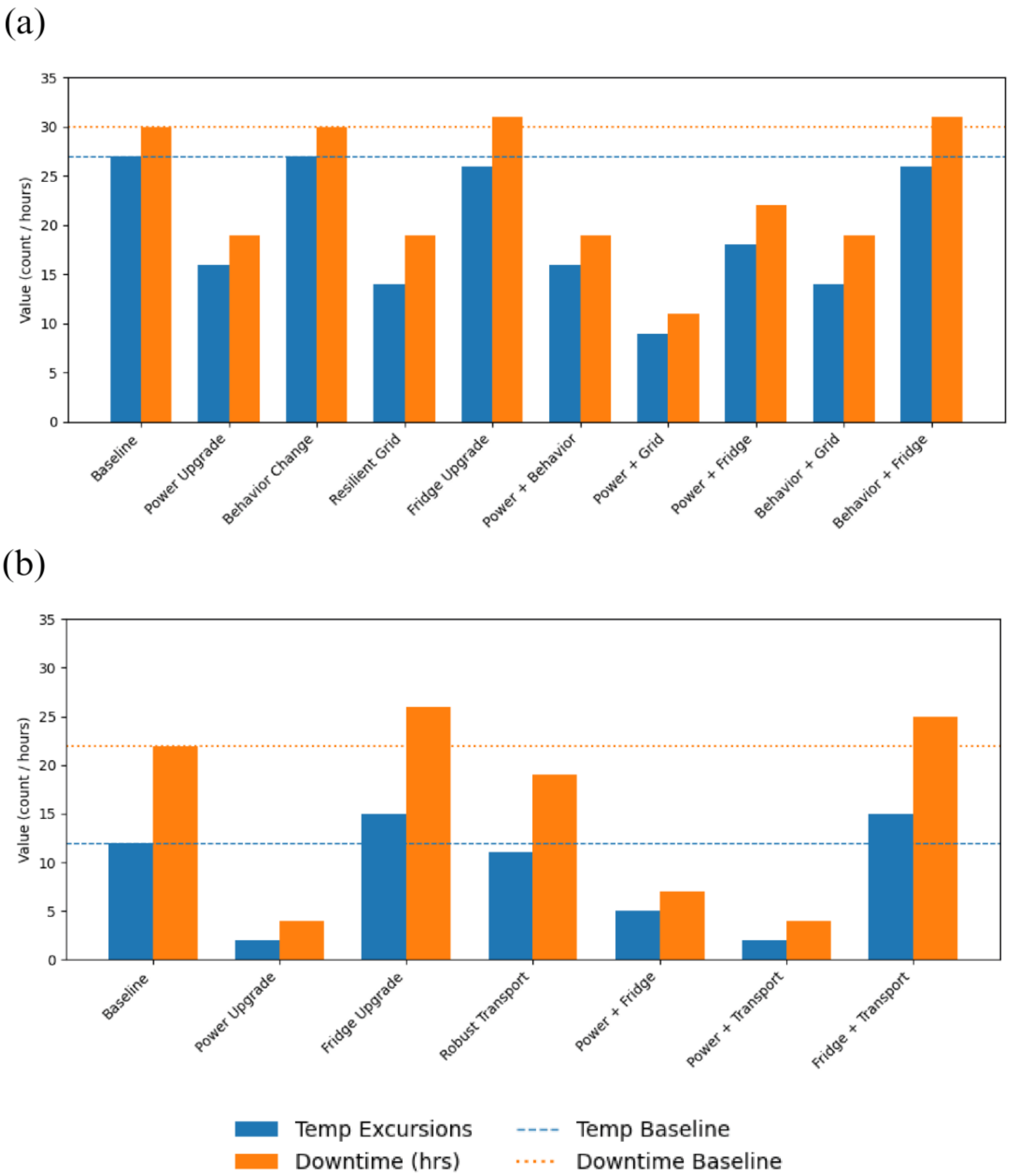

Figure 8. Effects of baseline and intervention scenarios on temperature excursions (left bars) and refrigeration downtime (right bars) in (a) Gaza and (b) rural Sudan. Horizontal reference lines indicate baseline performance for each metric. Bars below the corresponding baseline line represent improvements, while bars above indicate degraded performance. In both settings, interventions targeting power system reliability (e.g., power upgrades and resilient grid) produce the most consistent reductions in excursions and downtime. By contrast, isolated refrigeration upgrades show limited or negative effects, particularly in Sudan.

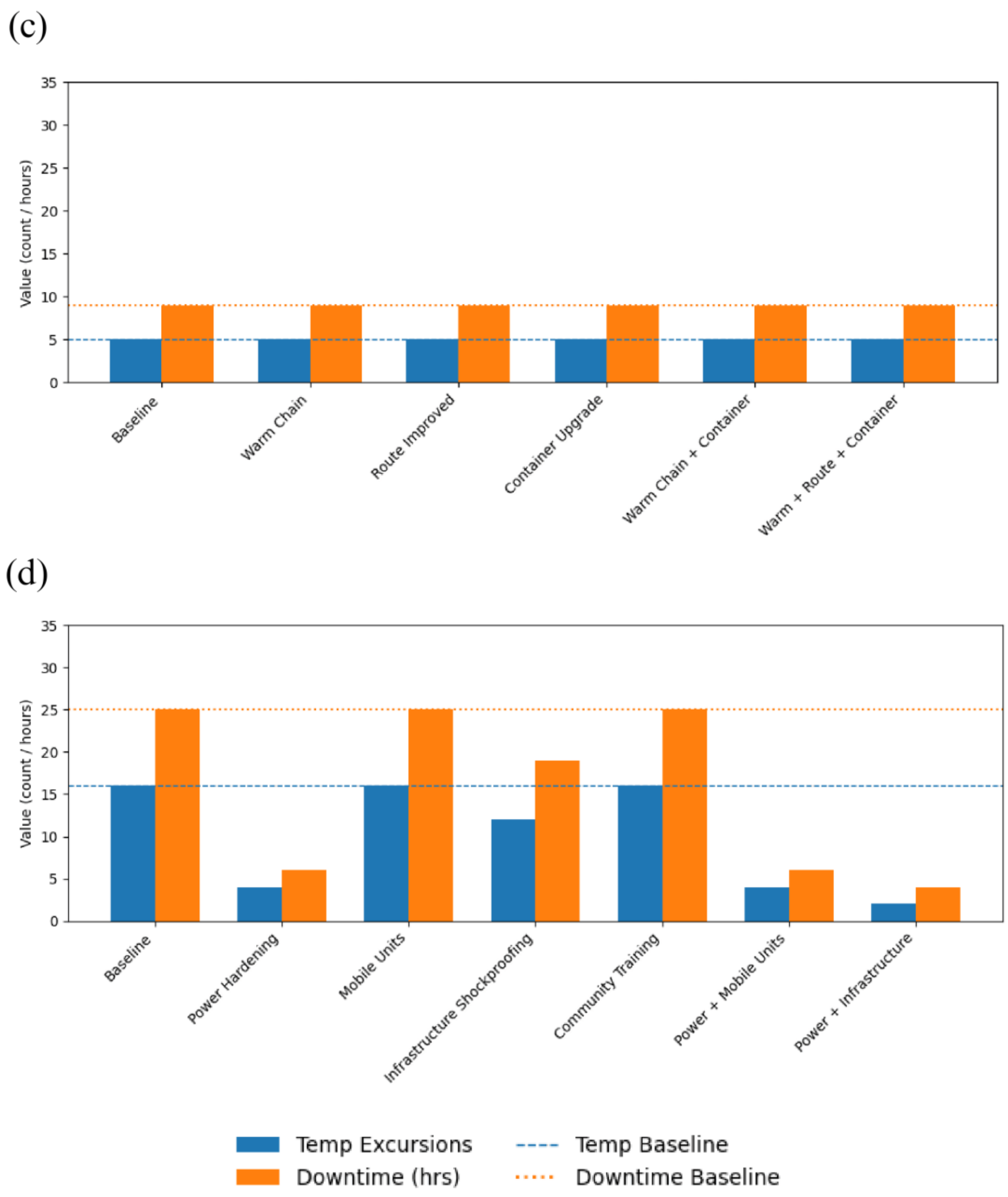

Figure 9. Effects of baseline and intervention scenarios on temperature excursions (left bars) and refrigeration downtime (right bars) in (c) Nepal Highlands and (d) post-earthquake Haiti. Horizontal reference lines indicate baseline performance for each metric. Bars below the baseline represent improvements relative to baseline conditions. In contrast to Figure 8, intervention effects are limited or highly selective in these settings. Nepal shows near-invariant performance across all interventions. Haiti exhibits moderate improvements primarily from power-focused interventions (e.g., power hardening and infrastructure shockproofing), while other measures yield minimal impact.

5 Discussion

The study's two research questions, whether vulnerability patterns are revealed by the integrated ABM–discrete–event framework (RQ1) and how context affects intervention effectiveness (RQ2), were used to interpret simulation experiments.

5.1 Findings for RQ1: Insights from Integrated Hybrid Simulation

RQ1 investigated whether a hybrid simulation integrating thermal, energy, logistical, and behavioral processes could reveal vulnerability patterns missed by conventional models. The results show that the framework captures interaction-driven and non-linear vulnerabilities that remain structurally obscured in static reliability or waste-rate approaches. Two findings illustrate this. First, equipment upgrades, typically assumed to improve performance, occasionally produced adverse outcomes in fragile environments by increasing energy demand beyond local grid capacity, thereby accelerating system instability rather than mitigating it, consistent with broader evidence that efficiency improvements can produce unintended system-level effects (Azevedo, 2014; Bahinipati et al., 2022; Gillingham et al., 2016). Second, vulnerability differed across inventory types under identical conditions: while standard 2–8°C items remained viable, vaccines with stricter temperature requirements (e.g., polio) consistently spoiled, reflecting the interaction between item-specific degradation kinetics and system temperature dynamics. Failures emerged from the coupling of thermal processes, energy availability, ambient conditions, and operational timing, particularly when delays in repair or refueling caused recovery, even when technically feasible, to be deferred due to temporal misalignment between thermal stress and response timing. These interaction effects are not captured in conventional models that treat temperature exposure as exogenous or rely on fixed wastage rates.

5.2 Findings for RQ2: Context Dependence of Intervention Performance

RQ2 investigated how interventions performed across different humanitarian settings. The results indicate that intervention efficacy was not an intrinsic property of the technology or policy itself, but was strongly shaped by the primary binding constraints of each specific context.

Infrastructure interventions, such as backup power and grid hardening, were most effective where energy insecurity constituted the dominant bottleneck. In the Gaza, Sudan, and Haiti archetypes, these measures reduced system downtime by approximately 35–80% relative to baseline, varying by context (e.g., from 30 to 19 hours in Gaza, 22 to 4 hours in Sudan, and 25 to 6 hours in Haiti). Conversely, in the Nepal Highlands, where terrain-driven transport delays were the primary constraint, identical energy interventions produced no observable improvement (0% change in downtime), indicating that when logistics, rather than energy, is the binding constraint, power upgrades yield no marginal system benefit within the modeled conditions.

A key counterintuitive finding involved technical equipment upgrades. In fragile energy settings, such as the rural Sudan archetype, upgraded fridges increased energy demand beyond the capacity of local energy systems, accelerating depletion and prolonging recovery (e.g., from 22 to 26 hours, ~18% increase; with smaller but consistent increases also observed in Gaza). These results challenge the notion of a "technological fix"—the tendency to treat hardware upgrades as primary solutions to structurally rooted vulnerabilities (Sætra & Selinger, 2024), suggesting instead that infrastructure robustness may need to precede or accompany equipment upgrades for technical benefits to materialize.

Under the modeled stress conditions, behavioral and operational interventions, such as reduced door openings, acted as secondary or complementary measures. As standalone strategies, their effects remained limited and did not exceed the reductions achieved through power and infrastructure improvements, even when combined with them. This pattern suggests a context-dependent structuring of constraints within the system: physical and energy limitations define the performance envelope, while behavioral adjustments influence outcomes within that envelope, aligning with prior cold-chain and supply-system findings that identify infrastructure reliability and logistical constraints as primary determinants of temperature control performance (Fahrni et al., 2022; Jaelani et al., 2025).

5.3 Comparison with Prior Work

Compared with the cold-chain modeling literature reviewed in Section 2.4, the main contribution of this study is not improved allocation or routing efficiency, but the generation of thermal failure as an emergent consequence of interacting factors. In prior cold-chain simulation work, such as Haidari et al.'s HERMES studies, relieving one bottleneck can shift stress downstream rather than remove it, and outages are often treated as thresholds for equipment choice rather than as dynamic processes that can invalidate a distribution plan (Haidari et al., 2013a, 2013b; Haidari et al., 2017). Similarly, optimization and resilience models improve location, inventory, and routing decisions under uncertainty, and typically treat thermal feasibility as an imposed condition, whereas the present framework models it as an emergent state arising from interacting power, thermal, environmental, and operational processes (Goodarzian et al., 2023; Kamran et al., 2023; Manupati et al., 2021; Tirkolaee et al., 2023). Stability-focused studies estimate potency loss from prescribed temperature profiles, while humanitarian logistics models evaluate cost, coverage, and response time (Ahmadi et al., 2015; Faria et al., 2022; Miura, 2024; Quispe et al., 2024). In contrast, the present framework explicitly models temperature exposure as emerging from these interactions, shifting the modeled endpoint from delivery performance to physical usability. By integrating these subsystems, the framework connects the prescriptive focus of cold-chain guidelines with the observed effects of combined stressors in practice. In this sense, the study sits between prescription and observation.

The mechanisms identified in this study are partially echoed in prior engineering and empirical studies, which independently show that increased cooling capacity can strain limited power supplies (Chandan et al., 2012; Strofer et al., 2023), passive buffering has finite holdover (Billah et al., 2016; Ng et al., 2020), and operational gaps can amplify short disturbances into spoilage (Pradeep et al., 2021; Rao et al., 2012; Sinha et al., 2017); however, these effects are typically observed in isolation across different contexts, whereas the present framework represents them as coupled, dynamic interactions within a single cold-chain system.

5.4 Limitations and Scope for Future Work

This study was simulation-based and therefore dependent on model structure, abstraction choices, and parameters. The framework is intended as a diagnostic stress-testing tool for exploring interaction-driven vulnerabilities rather than as a predictive or field-calibrated model. Its results are therefore best interpreted comparatively and mechanistically, rather than as inputs to site-specific forecasting or deployment decisions.

Parameter uncertainty is an inherent constraint. Scenarios were parameterized using plausible ranges informed by the literature, and robustness was assessed through targeted one-at-a-time sensitivity checks. While these analyses identified dominant drivers, they do not cover the full high-dimensional uncertainty space. More comprehensive global sensitivity analysis, probabilistic calibration, and decision-robustness evaluation remain important extensions.

Human and operational behavior were represented through simplified, stochastic, state-based agents rather than empirically calibrated decision models. This abstraction captured variability and delayed response but could not fully represent the social, institutional, and political dynamics that shape real-world operations. Disruption processes were likewise modeled in stylized form; in practice, outages, delays, and failures can arise from interacting infrastructural, regulatory, geopolitical, and environmental factors that could generate cascading effects beyond the present scope.

The aggregated outcome metrics used for comparative analysis focused on thermal excursions, cumulative exposure, downtime, spoilage, and delivery success. Other relevant considerations, such as cost, equity, downstream health impacts, and competing energy demands, were not included. Intervention experiments were exploratory and comparative rather than cost-optimal, and extending the framework to include economic evaluation, health impact metrics, or integrated optimization remains an important direction for future work.

Finally, the four scenarios represented stylized fragility archetypes rather than calibrated national case studies. While regional reports and operational evidence informed scenario configuration and parameter ranges, geographic labels were used to convey contrasting stress profiles rather than to make claims about specific locations. Findings should therefore be transferred cautiously by re-parameterizing the framework to local conditions and, where feasible, validating against monitoring or field data. Together, these limitations clarify the framework's intended role as a comparative, process-level tool for examining interaction-driven vulnerability under stress.

6 Conclusions

This study introduced a hybrid simulation framework that integrates thermal dynamics, power availability, logistics, operational behavior, stochastic disruptions, and temperature-dependent spoilage processes to examine cold-chain behavior under stress in humanitarian and resource-constrained settings. Across the modeled scenarios, temperature excursions and spoilage risk were observed to concentrate at specific system interfaces, particularly at clinic-level storage, during transport with limited thermal buffering, and under unstable power conditions.

The results further indicate that system behavior under disruption is shaped by interactions across subsystems rather than by isolated component functioning. Intervention effects varied across scenarios, with measures affecting energy availability and system configuration influencing outcomes more than standalone equipment or behavioral changes. Taken together, these findings underscore the importance of analyzing cold chains as coupled operational systems when examining system behavior under stress.

Funding

No external funding was received for this research.

Data/Software Access Statement

Supplementary materials and simulation code are available in public repositories. The simulation framework is available on GitHub, with a versioned archival snapshot (v1.0.1) available on Zenodo (https://doi.org/10.5281/zenodo.20976107). Additional supplementary materials, including spoilage model results, parameter configurations, and power utilization outputs, are available in a separate Zenodo repository (https://doi.org/10.5281/zenodo.17281048).

Contributor Statement

The author contributed to Conceptualization, Methodology, Software, Data Curation, Formal Analysis, Validation, Visualization, Writing – Original Draft, Writing – Review & Editing, and Project Administration.

Use of AI

During the preparation of this work, ChatGPT and Grammarly were used to rephrase certain paragraphs and improve clarity and readability. After using these tools, the author reviewed, edited, and validated all content as needed and takes full responsibility for the final publication.

Conflict Of Interest (COI)

There is no conflict of interest.

References

Ahmadi, M., Seifi, A., & Tootooni, B. (2015). A humanitarian logistics model for disaster relief operation considering network failure and standard relief time: A case study on San Francisco district. *Transportation Research Part E: Logistics and Transportation Review*, *75*, 145–163. https://doi.org/10.1016/j.tre.2015.01.008

AKCP. (2021). *Preventing cold chain failures using remote monitoring systems*. https://www.environmental-expert.com/articles/preventing-cold-chain-failures-using-remote-monitoring-systems-1012416

Ayowole, D. J., Adebajo, G. O., Lasisi, T. O., & Bakai, J. G. (2025). Effects of climate change on vaccine storage and cold chain logistics: a qualitative study in Ogun State, Nigeria. *BMJ Global Health*, *10*(7), e018990. https://doi.org/10.1136/bmjgh-2025-018990

Azevedo, I. M. L. (2014). Consumer End-Use Energy Efficiency and Rebound Effects. *Annual Review of Environment and Resources*, *39*(1), 393–418. https://doi.org/10.1146/annurev-environ-021913-153558

Bahinipati, C. S., Sirohi, R. A., & Rao, S. S. (2022). Technological Innovations, Behavioural Interventions, and Household Energy Conservation. *Ecology, Economy and Society–the INSEE Journal*, *5*(1). https://doi.org/10.37773/ees.v5i1.530

Bajrovic, I., & Croyle, M. A. (2023). Challenges in vaccine transport: can we deliver without the cold chain? *Expert Review of Vaccines*, *22*(1), 933–936. https://doi.org/10.1080/14760584.2023.2273901

Billah, M. M., Zaman, K., Estivariz, C. F., Snider, C. J., Anand, A., Hampton, L. M., Bari, T. I. A., Russell, K. L., & Chai, S. J. (2016). Cold-Chain adaptability during introduction of inactivated polio vaccine in Bangladesh, 2015. *The Journal of Infectious Diseases*, *216*(suppl_1), S114–S121. https://doi.org/10.1093/infdis/jiw591

Bruneau, M., & Reinhorn, A. (2006). *Overview of the resilience concept*. https://www.eng.buffalo.edu/~bruneau/8NCEE-Bruneau%20Reinhorn%20Resilience.pdf

Campa, C., Pronce, T., Paludi, M., Weusten, J., Conway, L., Savery, J., Richards, C., & Clénet, D. (2021). Use of stability modeling to support accelerated vaccine development and supply. *Vaccines*, *9*(10), 1114. https://doi.org/10.3390/vaccines9101114

Centers for Disease Control and Prevention. (2024). *Vaccine storage and handling*. https://www.cdc.gov/vaccines/hcp/storage-handling/index.html

Chandan, V., Do, A.-T., Jin, B., Jabbari, F., Brouwer, J., Akrotirianakis, I., Chakraborty, A., & Alleyne, A. (2012). Modeling and optimization of a combined cooling, heating and power plant system. 2012 American Control Conference (ACC), 3069–3074. https://doi.org/10.1109/ACC.2012.6315606

Chen, Y., Chen, M., & Hu, T. (2025). Designing a sustainable-resilient vaccine cold chain network in uncertain environments. *Computers & Chemical Engineering*, *194*, 108936. https://doi.org/10.1016/j.compchemeng.2024.108936

Chukwuka, O. J., Ren, J., Wang, J., & Paraskevadakis, D. (2024). Managing risk in emergency supply chains – An empirical study. *International Journal of Logistics Research and Applications*, *28*(9), 1072–1108. https://doi.org/10.1080/13675567.2024.2359645

Clénet, D. (2018). Accurate prediction of vaccine stability under real storage conditions and during temperature excursions. *European Journal of Pharmaceutics and Biopharmaceutics*, *125*, 76–84. https://doi.org/10.1016/j.ejpb.2018.01.005

Comes, T., Sandvik, K. B., & Van De Walle, B. (2018). Cold chains, interrupted. *Journal of Humanitarian Logistics and Supply Chain Management*, *8*(1), 49–69. https://doi.org/10.1108/jhlscm-03-2017-0006

De Luca, G., Lampoltshammer, T. J., Parven, S., & Scholz, J. (2022). A literature review on the usage of Agent-Based Modelling to study policies for managing international migration. *Social Sciences*, *11*(8), 356. https://doi.org/10.3390/socsci11080356

Fahrni, M. L., Ismail, I. A.-N., Refi, D. M., Almeman, A., Yaakob, N. C., Saman, K. M., Mansor, N. F., Noordin, N., & Babar, Z.-U.-D. (2022). Management of COVID-19 vaccines cold chain logistics: a scoping review. *Journal of Pharmaceutical Policy and Practice*, *15*(1), 16. https://doi.org/10.1186/s40545-022-00411-5

Fan, Y., de Kleuver, C., de Leeuw, S., & Behdani, B. (2021). Trading off cost, emission, and quality in cold chain design: A simulation approach. *Computers & Industrial Engineering*, *158*, 107442. https://doi.org/10.1016/j.cie.2021.107442

Faria, M., Palhares, L. A. M., Souza, D. A., & Lopes, R. B. (2022). What would be representative temperatures for shelf-life studies with biopesticides in tropical countries? Estimates through long-term storage of biocontrol fungi and calculation of mean kinetic temperatures. *BioControl*, *67*(2), 213–224. https://doi.org/10.1007/s10526-021-10126-2

Feyisa, D., Jemal, A., Aferu, T., Ejeta, F., & Endeshaw, A. (2021). Evaluation of Cold Chain Management Performance for Temperature-Sensitive Pharmaceuticals at Public Health Facilities Supplied by the Jimma Pharmaceuticals Supply Agency Hub, Southwest Ethiopia: Pharmaceuticals Logistic Management Perspective Using a Multicentered, Mixed-Method Approach. *Advances in Pharmacological and Pharmaceutical Sciences*, *2021*, 1–13. https://doi.org/10.1155/2021/5167858

Gillingham, K., Rapson, D., & Wagner, G. (2016). The Rebound Effect and Energy Efficiency Policy. *Review of Environmental Economics and Policy*, *10*(1), 68–88. https://doi.org/10.1093/reep/rev017

Gligor, D., Tan, A., & Nguyen, T. N. T. (2018). The obstacles to cold chain implementation in developing countries: insights from Vietnam. *The International Journal of Logistics Management*, *29*(3), 942–958. https://doi.org/10.1108/ijlm-02-2017-0026

Goebel, A. (2024, December 3). *The importance of the cold chain in the pharma industry.* Advanco. https://www.advanco.com/article/the-importance-of-the-cold-chain-in-the-pharma-industry/

Goodarzian, F., Navaei, A., Ehsani, B., Ghasemi, P., & Muñuzuri, J. (2023). Designing an integrated responsive-green-cold vaccine supply chain network using Internet-of-Things: artificial intelligence-based solutions. *Annals of Operations Research*, *328*(1), 531–575. https://doi.org/10.1007/s10479-022-04713-4

Haidari, L. A., Connor, D. L., Wateska, A. R., Brown, S. T., Mueller, L. E., Norman, B. A., Schmitz, M. M., Paul, P., Rajgopal, J., Welling, J. S., Leonard, J., Chen, S.-I., & Lee, B. Y. (2013a). Augmenting Transport versus Increasing Cold Storage to Improve Vaccine Supply Chains. *PLoS ONE*, *8*(5), e64303. https://doi.org/10.1371/journal.pone.0064303

Haidari, L. A., Connor, D. L., Wateska, A. R., Brown, S. T., Mueller, L. E., Norman, B. A., Schmitz, M. M., Paul, P., Rajgopal, J., Welling, J. S., Leonard, J., Claypool, E. G., Weng, Y.-T., Chen, S.-I., & Lee, B. Y. (2013b). Only Adding Stationary Storage to Vaccine Supply Chains May Create and Worsen Transport Bottlenecks. *Journal* *of Public Health Management and Practice*, *19*(Supplement 2), S65–S67. https://doi.org/10.1097/PHH.0b013e31828a83fe

Haidari, L. A., Brown, S. T., Wedlock, P., Connor, D. L., Spiker, M., & Lee, B. Y. (2017). When are solar refrigerators less costly than on-grid refrigerators: A simulation modeling study. *Vaccine, 35*(17), 2224–2228. https://doi.org/10.1016/j.vaccine.2016.11.103

Hay, M., Teichert, A., Kilz, S., & Vosen, A. (2025). Resilience in the Vaccine Supply Chain: Learning from the COVID-19 Pandemic. *Vaccines*, *13*(2), 142. https://doi.org/10.3390/vaccines13020142

Hemmeda, L., Ahmed, A. S., & Omer, M. (2023). Sudan's armed rivalry: A comment on the vulnerable healthcare system catastrophe. *Health Science Reports*, *6*(8). https://doi.org/10.1002/hsr2.1517

Hemmeda, L., Tiwari, A., Kolawole, B. O., Ayoobkhan, F. S., Fatima, K., Shabani, M. M., Kundu, M., Anugu, N. R., Richard, R. M., Ibrahim, D., & Ahmed, K. A. H. M. (2024). The critical pharmaceutical situation in Sudan 2023: A humanitarian catastrophe of civil war. *International Journal for Equity in Health*, *23*(1). https://doi.org/10.1186/s12939-024-02103-9

Human Rights Watch. (2024). *Israel and Palestine: Events of 2023*. https://www.hrw.org/world-report/2024/country-chapters/israel-and-palestine

Işık, E. E., & Yildiz, S. T. (2023). Optimizing the COVID-19 cold chain vaccine distribution network with medical waste management: A robust optimization approach. *Expert Systems with Applications*, *229*, 120510. https://doi.org/10.1016/j.eswa.2023.120510

Jaelani, I., Harsanto, B., Azis, Y., Sari, D., & Kaltum, U. (2025). Cold chain logistics challenges on sustainability: A systematic review. *Sustainable Futures*, *10*, 101559. https://doi.org/10.1016/j.sftr.2025.101559

Jenkins, D., Cancel, A., & Layloff, T. (2022). Mean kinetic temperature evaluations through simulated temperature excursions and risk assessment with oral dosage usage for health programs. *BMC Public Health*, *22*(1). https://doi.org/10.1186/s12889-022-12660-9

De Boeck, K., Decouttere, C., & Vandaele, N. (2018). Vaccine distribution supply chains in developing countries: A literature review. *Ideas.Repec.Org*. https://ideas.repec.org/p/ete/kbiper/629348.html

Kamran, M. A., Kia, R., Goodarzian, F., & Ghasemi, P. (2023). A new vaccine supply chain network under COVID-19 conditions considering system dynamic: Artificial intelligence algorithms. *Socio-Economic Planning Sciences*, *85*, 101378. https://doi.org/10.1016/j.seps.2022.101378

Kargar, B., MohajerAnsari, P., Büyüktahtakın, İ. E., Jahani, H., & Talluri, S. (2024). Data-driven modeling for designing a sustainable and efficient vaccine supply chain: A COVID-19 case study. *Transportation Research Part E Logistics and Transportation Review*, *184*, 103494. https://doi.org/10.1016/j.tre.2024.103494

Khalilpoor, S., Kamran, M. A., & Solimanpur, M. (2025). Resilient COVID-19 vaccine supply chain: An optimization and simulation approach for multi-objective management. *Transportation Research Part E Logistics and Transportation Review*, *201*, 104168. https://doi.org/10.1016/j.tre.2025.104168

Khodaee, V., Kayvanfar, V., & Haji, A. (2022). A humanitarian cold supply chain distribution model with equity consideration: The case of COVID-19 vaccine distribution in the European Union. *Decision Analytics Journal*, *4*, 100126. https://doi.org/10.1016/j.dajour.2022.100126

Kim, J. J., Jang, H., & Roh, S. (2022). A systematic literature review on humanitarian logistics using network analysis and topic modeling. *The Asian Journal of Shipping and Logistics*, *38*(4), 263–278. https://doi.org/10.1016/j.ajsl.2022.10.003

Kruczkiewicz, A., Klopp, J., Fisher, J., Mason, S., McClain, S., Sheekh, N. M., Moss, R., Parks, R. M., & Braneon, C. (2021). Compound risks and complex emergencies require new approaches to preparedness. *Proceedings of the National Academy of Sciences*, *118*(19). https://doi.org/10.1073/pnas.2106795118

Kruk, M. E., Myers, M., Varpilah, S. T., & Dahn, B. T. (2015). What is a resilient health system? Lessons from Ebola. *The Lancet*, *385*(9980), 1910–1912. https://doi.org/10.1016/s0140-6736(15)60755-3

Lee, B. Y., Haidari, L. A., Prosser, W., Connor, D. L., Bechtel, R., Dipuve, A., Kassim, H., Khanlawia, B., & Brown, S. T. (2016). Re-designing the Mozambique vaccine supply chain to improve access to vaccines. *Vaccine*, *34*(41), 4998–5004. https://doi.org/10.1016/j.vaccine.2016.08.036

Li, F., Tao, J., Wang, Q., Guo, W., Wang, X., Wang, B., Su, H., Cheng, Z., Yan, B., & Chen, G. (2025). Simulation and optimization of cold chain logistics system towards lower carbon emission: a state-of-the-art review. *Carbon Research*, *4*(1), 22. https://doi.org/10.1007/s44246-024-00191-4

Linkov, I., Eisenberg, D. A., Plourde, K., Seager, T. P., Allen, J., & Kott, A. (2013). Resilience metrics for cyber systems. *Environment Systems & Decisions*, *33*(4), 471–476. https://doi.org/10.1007/s10669-013-9485-y

Manupati, V. K., Schoenherr, T., Subramanian, N., Ramkumar, M., Soni, B., & Panigrahi, S. (2021). A multi-echelon dynamic cold chain for managing vaccine distribution. *Transportation Research Part E: Logistics and Transportation Review*, *156*, 102542. https://doi.org/10.1016/j.tre.2021.102542

Marchi, B., & Zanoni, S. (2022). Cold Chain Energy Analysis for Sustainable Food and Beverage Supply. *Sustainability*, *14*(18), 11137. https://doi.org/10.3390/su141811137

Médecins Sans Frontières. (2025). *Mali: Disruptions to fuel supplies impact MSF medical activities*. https://www.msf.org/mali-disruptions-fuel-supplies-impact-msf-medical-activities

Medicine Quality Research Group (2021). *Medical Product Quality Report – COVID-19 issues. Issue 14, Data from October, November & December 2021*. Medicine Quality Research Group, University of Oxford. https://www.iddo.org/document/medical-product-quality-report-covid-19-issues-issue-14-april-2022-data-october-december

Mirai Intex. (2024). *Pharma cold chain: pharmaceutical cold storage, managment and logstics*. https://mirai-intex.com/blog/cold-chain-in-the-pharmaceutical-industry-ensuring-safe-and-effective-medications

Miura, E. (2024). Use of Mean Kinetic Temperature for Pharmaceuticals in Japan and Stability Monitoring in the 21st Century. *Therapeutic Innovation & Regulatory Science*, *58*(1), 184–191. https://doi.org/10.1007/s43441-023-00584-4

Mohammed, A., James, P., & Bahaj, A. (2025). Electricity access linkages to sustainable development goals in rural Sudan. *Sustainability*, *17*(6), 2441. https://doi.org/10.3390/su17062441

Mueller, L. E., Haidari, L. A., Wateska, A. R., Phillips, R. J., Schmitz, M. M., Connor, D. L., Norman, B. A., Brown, S. T., Welling, J. S., & Lee, B. Y. (2016). The impact of implementing a demand forecasting system into a low-income country's supply chain. *Vaccine*, *34*(32), 3663–3669. https://doi.org/10.1016/j.vaccine.2016.05.027

Nepal Electricity Authority. (2025). *Annual report 2024/2025*. https://www.nea.org.np/admin/assets/uploads/supportive_docs/89899842.pdf

Ng, C. Z., Lean, Y. L., Yeoh, S. F., Lean, Q. Y., Lee, K. S., Suleiman, A. K., Liew, K. Bin, Kassab, Y. W., Al-Worafi, Y. M., & Ming, L. C. (2020). Cold chain time- and temperature-controlled transport of vaccines: a simulated experimental study. *Clinical and Experimental Vaccine Research*, *9*(1), 8. https://doi.org/10.7774/cevr.2020.9.1.8

OCHA. (n.d.). *Electricity in the Gaza Strip | United Nations Office for the Coordination of Humanitarian Affairs - Occupied Palestinian Territory*. Retrieved https://www.ochaopt.org/page/gaza-strip-electricity-supply

OCHA. (2023). *Occupied Palestinian Territory (FA) 2023 Flash Appeal: from 01/10/2023 to 31/12/2023*. https://humanitarianaction.info/plan/1186/article/opt-fa-2023

OCHA. (2025a). *Humanitarian situation Update #300: Gaza Strip*. https://www.ochaopt.org/content/humanitarian-situation-update-300-gaza-strip

OCHA. (2025b). *Humanitarian Situation Update #326 | Gaza Strip*. https://www.unocha.org/publications/report/occupied-palestinian-territory/humanitarian-situation-update-326-gaza-strip

Pradeep, P., Viral, S., Naresh, M., & Dipesh, P. (2021). Structure and process evaluation of cold chain management and routine immunization services in rural western Gujarat. *Journal of Basic and Applied Research in Biomedicine*, *6*(2), 70–74. https://doi.org/10.51152/jbarbiomed.v6i2.16

Quispe, M. F. C., Couto, A. S., De Brito Junior, I., Cunha, L. R. A., Siqueira, R. M., & Yoshizaki, H. T. Y. (2024). Humanitarian Logistics Prioritization Models: A Systematic Literature Review. *Logistics*, *8*(2), 60. https://doi.org/10.3390/logistics8020060

Rao, S., Naftar, S., Baliga, S., & Unnikrishnana, B. (2012). Evaluation, awareness, practice and management of cold chain at the primary health care centers in coastal South India. *Journal of Nepal Paediatric Society*, *32*(1), 19–22. https://doi.org/10.3126/jnps.v32i1.5946

Reuters. (2025). *Humanitarian operation in Myanmar hindered by damaged roads and infrastructure, says UN agency*. https://www.reuters.com/business/environment/humanitarian-operation-myanmar-hindered-by-damaged-roads-infrastructure-says-un-2025-03-29/

Sætra, H. S., & Selinger, E. (2024). Technological Remedies for Social Problems: Defining and Demarcating Techno-Fixes and Techno-Solutionism. *Science and Engineering Ethics*, *30*(6), 60. https://doi.org/10.1007/s11948-024-00524-x

Save the Children. (2023). *Sudan: Lifesaving vaccines for children destroyed in power outages amidst violence*. https://www.savethechildren.net/news/sudan-lifesaving-vaccines-children-destroyed-power-outages-amidst-violence

Scaccia, A., Saade, C., Ballesta, P., Rieger, M., & Clénet, D. (2025). Predicting stability of conventional and mRNA-based vaccines. *Vaccine Insights*, *4*(2), 27–39. https://doi.org/10.18609/vac.2025.054

SEBoK. (2025). *System Reliability, Availability, and Maintainability - SEBOK*. https://sebokwiki.org/wiki/System_Reliability%2C_Availability%2C_and_Maintainability

Sinha, A. K., Verma, A. R., Chandrakar, A., Khes, S. P., Panda, P. S., & Dixit, S. (2017). Evaluation of cold chain and logistics management practice in Durg district of Chhattisgarh: pointer from Central India. *International Journal of Community Medicine and Public Health*, *4*(2), 390. https://doi.org/10.18203/2394-6040.ijcmph20170260

Stoddard, A., Breckenridge, M.-J., Czwarno, M., & Duque-Díez, M. (2025). *Aid Worker Security Report 2025 – Defenceless: Aid worker security amid the humanitarian funding collapse*. Humanitarian Outcomes. https://humanitarianoutcomes.org/AWSR_2025

Strofer, C. M., Coe, R., Gaebele, D., Beringer, C., Bosma, B., Robertson, B., Bacelli, G., & Devin, M. (2023). Control co-design and uncertainty analysis of the LUPA's PTO using WecOptTool. *Proceedings of the European Wave and Tidal Energy Conference*, *15*. https://doi.org/10.36688/ewtec-2023-288

Tang, H. (2024). System performance metrics. In Manufacturing system throughput excellence: Analysis, improvement, and design (1st ed., pp. 33–70). Wiley. https://doi.org/10.1002/9781394190355.ch2

Tirkolaee, E. B., Torkayesh, A. E., Tavana, M., Goli, A., Simic, V., & Ding, W. (2023). An integrated decision support framework for resilient vaccine supply chain network design. *Engineering Applications of Artificial Intelligence*, *126*, 106945. https://doi.org/10.1016/j.engappai.2023.106945

UK Health Security Agency. (2013). *Storage, distribution and disposal of vaccines: the green book, chapter 3*. https://www.gov.uk/government/publications/storage-distribution-and-disposal-of-vaccines-the-green-book-chapter-3

UN Institute for Training and Research. (2022). *The state of the humanitarian energy Sector: Challenges, progress and issues in 2022*. https://reliefweb.int/report/world/state-humanitarian-energy-sector-challenges-progress-and-issues-2022

UNICEF. (n.d.). *Technical Review of Public Health Supply Chain Assessment tools: An analysis of major supply chain assessment tools and approaches*. Retrieved https://www.unicef.org/supply/documents/technical-review-public-health-supply-chain-assessment-tools

UNICEF. (2019). *Enhancing immunization programmes in Yemen*. https://www.unicef.org/yemen/stories/enhancing-immunization-programmes-yemen

UNICEF. (2021a). *E004 cold boxes and vaccine carriers*. https://www.unicef.org/supply/media/6391/file/VaccineCarrierColdBox-guideline-2021.pdf

UNICEF. (2021b). *Supply Chain Maturity Model Concept Note*. https://www.unicef.org/supply/documents/supply-chain-maturity-model-concept-note

United Nations Environment Programme. (2020). *Why optimized cold-chains could save a billion COVID vaccines*. https://www.unep.org/news-and-stories/story/why-optimized-cold-chains-could-save-billion-covid-vaccines

United Nations Office for the Coordination of Humanitarian Affairs. (2024). *Global Humanitarian Overview 2025 [EN/AR/FR/ES]*. https://www.unocha.org/publications/report/world/global-humanitarian-overview-2025-enarfres

Wang, Z., & Zhang, J. (2019). Agent-based evaluation of humanitarian relief goods supply capability. *International Journal of Disaster Risk Reduction*, *36*, 101105. https://doi.org/10.1016/j.ijdrr.2019.101105

World Health Organization (WHO). (n.d.). *Effective Vaccine Management (EVM)*. https://www.who.int/teams/immunization-vaccines-and-biologicals/essential-programme-on-immunization/supply-chain/effective-vaccine-management-(evm)

World Health Organization (WHO). (2015). *Vaccine Management Handbook: How to monitor temperatures in the vaccine supply chain*. https://www.who.int/publications/i/item/WHO-IVB-15.04

World Health Organization (WHO). (2018). *How to Develop a Continuous Improvement Plan (cIP)*. https://iris.who.int/bitstream/handle/10665/272861/9789241514293-eng.pdf

World Health Organization (WHO). (2023a). *Close to one billion people globally are served by health-care facilities with no electricity access or with unreliable electricity*. https://www.who.int/news/item/14-01-2023-close-to-one-billion-people-globally-are-served-by-health-care-facilities-with-no-electricity-access-or-with-unreliable-electricity

World Health Organization (WHO). (2023b). *Electricity in health-care facilities*. https://www.who.int/news-room/fact-sheets/detail/electricity-in-health-care-facilities

Pareja Yale, C. L., Lorena Da Silva Frazao, M., De Mesquita, M. A., & Yoshizaki, H. T. Y. (2020). Simulation Applications in Humanitarian Logistics: A Systematic Literature Review. *2020 Winter Simulation Conference (WSC)*, 2589–2600. https://doi.org/10.1109/WSC48552.2020.9384011

Appendix A.

A. Environmental & Power

Ambient temperature:

$$T_{\text{amb}}(t) = T_{\text{base}}(t) + \epsilon_{\text{daily}} + \epsilon_{\text{weather}}$$

Deterministic diurnal component:

$$T_{\text{base}}(t) = \begin{cases} T_{\text{night}} + \dfrac{\Delta T}{2}\left(1 - \cos\left(\dfrac{\pi(t - t_{\text{sr}})}{t_{\text{ss}} - t_{\text{sr}}}\right)\right), & t_{\text{sr}} \le t \le t_{\text{ss}}, \\ T_{\text{day}} e^{-\lambda\tau} + T_{\text{night}}\left(1 - e^{-\lambda\tau}\right), & \text{otherwise} \end{cases}$$

$$\epsilon_{\text{daily}} \sim \mathcal{U}(-1.5, 1.5)$$

$$\epsilon_{\text{weather}} = \begin{cases} -2, & p = 0.05 \\ +2, & p = 0.05 \\ 0, & p = 0.90 \end{cases}$$

Solar generation:

$$P_{\text{solar}}(t) = \begin{cases} A_{\text{panel}}\, I(t)\, \eta_{\text{panel}} \cos\left(\dfrac{\pi(h - 12)}{12}\right) \eta_{\text{tilt}}\, f_{\text{orient}}\, (1 - s_{\text{shade}})\, m_{\text{weather}}(t), & 6 \le h \le 18, \\ 0, & \text{otherwise} \end{cases}$$

Battery state update:

$$B(t + \Delta t) = \max\left\{E_{\text{cutoff}}(t),\ \min\left\{E_{\text{cap}}(t),\ B(t) + \eta_{\text{ch}} P_{\text{in}}(t)\Delta t - \frac{1}{\eta_{\text{dis}}} P_{\text{out}}(t)\Delta t\right\}\right\}$$

$$E_{\text{cutoff}}(t) = \alpha\, E_{\text{cap}}(t)$$

$$E_{\text{cap}}(t + \Delta t) = E_{\text{cap}}(t)\, (1 - \delta_{\text{cal}})^{\Delta t / t_{\text{week}}} \left(1 - \delta_{\text{cyc}}\right)^{N_{\text{cycles}}(t)}$$

Table A1. Symbols Used in the Environmental & Power Models

Symbol	Meaning	Unit
$T_{\text{amb}}(t)$	Ambient temperature	°C
$T_{\text{base}}(t)$	Deterministic diurnal temperature	°C
ϵ_{daily}	Daily stochastic variation	°C
$\epsilon_{\text{weather}}$	Weather perturbation	°C
$P_{\text{solar}}(t)$	Solar panel power output	W
A_{panel}	Solar panel area	m^2
$I(t)$	Solar irradiance	W/m^2
η_{panel}	Panel efficiency	–
η_{tilt}	Tilt efficiency factor	–
f_{orient}	Orientation factor	–
s_{shade}	Shading fraction	–
$m_{\text{weather}}(t)$	Weather modifier	–
$B(t)$	Battery state of charge	Wh
$E_{\text{cap}}(t)$	Battery capacity	Wh
$E_{\text{cutoff}}(t)$	Minimum battery cutoff	Wh
η_{ch}	Battery charging efficiency	–
η_{dis}	Battery discharging efficiency	–
$P_{\text{in}}(t)$	Power into battery	W
$P_{\text{out}}(t)$	Power drawn from battery	W

B. Hierarchical Power Dispatch

B.1 Residual-Demand Formulation

Initial demand:

$$R_0(t) = P_{\text{load}}(t)$$

Sequential source dispatch:

$$P_i(t) = \min\left(P_i^{\max}(t), R_{i-1}(t)\right), \qquad R_i(t) = R_{i-1}(t) - P_i(t)$$

with priority order

$$i \in \{\text{grid, solar, battery, gen}\}.$$

B.2 Total Supplied Power

$$P_{\text{supplied}}(t) = \sum_i P_i\,(t)$$

B.3 Unserved Demand

$$P_{\text{unserved}}(t) = \max\left(0,\, P_{\text{load}}(t) - P_{\text{supplied}}(t)\right)$$

B.4 Opportunistic Battery Charging

$$\Delta E_{\text{charge}}(t) = \begin{cases} \eta_{\text{ch}} \min\left(P_{\text{charge}}^{\max}, P_{\text{grid}}^{\text{excess}}(t)\right) \Delta t, & \text{if grid available,} \\ \eta_{\text{ch}} P_{\text{solar}}^{\text{excess}}(t) \Delta t, & \text{otherwise if solar available.} \end{cases}$$

Table A2. Symbols Used in the Hierarchical Power Dispatch Model

Symbol	Meaning	Unit
$P_{\text{load}}(t)$	Total load demand	W
$R_0(t)$	Initial residual demand	W
$P_i(t)$	Power supplied by source i	W
$P_i^{\max}(t)$	Maximum available power from source i	W
$R_i(t)$	Residual demand after source i	W
i	Power source index	–
$P_{\text{supplied}}(t)$	Total supplied power	W
$P_{\text{unserved}}(t)$	Power demand not served (blackout)	W
$\Delta E_{\text{charge}}(t)$	Energy charged into battery	Wh
η_{ch}	Battery charging efficiency	–
$P_{\text{charge}}^{\max}$	Max battery charging rate	W
$P_{\text{grid}}^{\text{excess}}(t)$	Grid power beyond load	W
$P_{\text{solar}}^{\text{excess}}(t)$	Solar power beyond load	W

C. Refrigeration / Thermal Dynamics

C.1 Temperature State Update

$$T_{\text{fr}}(t + \Delta t) = T_{\text{fr}}(t) + \frac{\Delta t}{C_{\text{th}}}[Q_{\text{cond}}(t) + Q_{\text{infiltration}}(t) - P_{\text{cool}}(t)] + \Delta T_{\text{door}}(t) + \Delta T_{\text{items}}(t)$$

C.2 Heat Transfer Mechanisms

Conduction through insulation

$$Q_{\text{cond}}(t) = \frac{T_{\text{amb}}(t) - T_{\text{fr}}(t)}{R}$$

Continuous air infiltration

$$Q_{\text{infiltration}}(t) = \rho_{\text{air}}\, c_{p,\text{air}}\, V\, \text{ACH}\big(T_{\text{amb}}(t) - T_{\text{fr}}(t)\big)$$

C.3 Thermostatic Compressor Control

$$P_{\text{cool}}(t) = \begin{cases} \min\left(P_{\text{rated}}, \dfrac{C_{\text{th}}(T_{\text{fr}}(t) - T_{\min})}{\Delta t}\right), & \mathbb{1}_{\text{power}}(t) = 1 \text{ and } T_{\text{fr}}(t) > T_{\max}, \\ 0, & \text{otherwise.} \end{cases}$$

C.4 Door Opening Thermal Impulse

$$\Delta T_{\mathrm{door}}(t) = \min\left\{\frac{\rho_{\mathrm{air}}\, c_{p,\mathrm{air}}\, V\, f_{\mathrm{ex}}(\tau)\big(T_{\mathrm{amb}}(t) - T_{\mathrm{fr}}(t)\big)}{C_{\mathrm{th}}},\ \gamma_{\max}\frac{\tau}{60}\right\}$$

$$f_{\mathrm{ex}}(\tau) = \min\left(0.95,\ 0.1 + \frac{0.15}{60}\tau\right).$$

C.5 Inserted Item Thermal Impulse

$$\Delta T_{\mathrm{items}}(t) = \frac{m_{\mathrm{item}}\, c_{p,\mathrm{item}}\,\big(T_{\mathrm{item}} - T_{\mathrm{fr}}(t)\big)}{C_{\mathrm{th}} + m_{\mathrm{item}}\, c_{p,\mathrm{item}}}$$

Table A3. Symbols Used in the Refrigerator Thermal Model

Symbol	Meaning	Unit
$T_{\mathrm{fr}}(t)$	Internal refrigerator temperature	°C
$T_{\mathrm{amb}}(t)$	Ambient temperature	°C
C_{th}	Thermal capacitance	J/°C
R	Thermal resistance	°C/W
$P_{\mathrm{cool}}(t)$	Cooling power	W
P_{rated}	Rated compressor power	W
$T_{\min}, T_{\max}$	Thermostat bounds	°C
ρ_{air}	Air density	kg/m³
$c_{p,\mathrm{air}}$	Air specific heat	J/(kg·°C)
V	Fridge volume	m³
ACH	Air change rate	h⁻¹
$f_{\mathrm{ex}}(\tau)$	Door air-exchange fraction	–
$\gamma_{\max}$	Door warming limiter	°C/min
m_{item}	Inserted item mass	kg
$c_{p,\mathrm{item}}$	Item specific heat	J/(kg·°C)
T_{item}	Item initial temperature	°C

D. Spoilage / Product-Stability Models

D.1 Cumulative Exposure Model

$$E_{\mathrm{time}}(t) = \sum_{\{i \mid T_i \notin [T_{\min}, T_{\max}]\}} \Delta t_i$$

$$S_{\mathrm{cumulative}}(t) = \mathbb{1}\{E_{\mathrm{time}}(t) \ge t_{\max}\}$$

D.2 Thermal Stress Model

$$\Theta(t) = \sum \max(0,\ T_{\mathrm{fr}}(t) - T_{\mathrm{safe}})\Delta t$$

$$S_{\mathrm{thermal}}(t) = \mathbb{1}\{\Theta(t) \ge \Theta_{\mathrm{crit}}\}$$

D.3 Arrhenius Model

$$k(T) = A\exp\left(-\frac{E_a}{R_u(T + 273.15)}\right)$$

$$D(t + \Delta t) = D(t) + k\big(T(t)\big)\,\Delta t$$

$$S_{\text{arrhenius}}(t) = \mathbb{1}\{D(t) \geq 1\}$$

Table A4. Symbols Used in the Spoilage Models

Symbol	Meaning	Unit
$T_{\text{fr}}(t)$	Storage temperature	°C
$T_{\min}, T_{\max}$	Safe temperature bounds	°C
$E_{\text{time}}(t)$	Cumulative time outside safe range	h
$t_{\max}$	Maximum allowed cumulative exposure time	h
$\Theta(t)$	Thermal stress integral	°C·h
T_{safe}	Reference safe temperature	°C
Θ_{crit}	Critical thermal stress threshold	°C·h
$k(T)$	Temperature-dependent degradation rate	h^{-1}
A	Pre-exponential factor	h^{-1}
E_a	Activation energy	J/mol
R_u	Universal gas constant	J/(mol·K)
$D(t)$	Accumulated degradation damage	–
$S_{\text{cumulative}}$	Cumulative spoilage indicator	–
S_{thermal}	Thermal stress spoilage indicator	–
$S_{\text{arrhenius}}$	Arrhenius spoilage indicator	–

E. Transport Thermal Model

E.1 Passive Transport (Cold Box)

Heat inflow:

$$\dot{Q}_{\text{in}}(t) = \frac{T_{\text{amb}}(t) - T_{\text{unit}}(t)}{R_{\text{unit}}}$$

Ice energy depletion:

$$E_{\text{ice}}(t + \Delta t) = \max\{E_{\text{ice}}(t) - \dot{Q}_{\text{in}}(t)\,\Delta t,\, 0\}$$

Temperature update:

$$T_{\text{unit}}(t + \Delta t) = \begin{cases} T_{\text{unit}}(t), & E_{\text{ice}}(t) > 0, \\ T_{\text{unit}}(t) + \dfrac{\Delta t}{C_{\text{unit}}}\,\dfrac{T_{\text{amb}}(t) - T_{\text{unit}}(t)}{R_{\text{unit}}}, & E_{\text{ice}}(t) = 0. \end{cases}$$

Post-melt clamping:

$$T_{\text{unit}}(t) \leftarrow \min\{T_{\text{unit}}(t), T_{\text{amb}}(t) + 2\} \quad \text{if } E_{\text{ice}}(t) = 0$$

E.2 Active Transport

$$T_{\text{unit}}(t + \Delta t) = T_{\text{fr}}(t + \Delta t)$$

E.3 Re-icing Operation

$$E_{\text{ice}} \leftarrow m_{\text{ice}} L_f$$

$$T_{\text{unit}} \leftarrow T_{\text{reset}}$$

Table A5. Symbols Used in the Transport Thermal Model

Symbol	Meaning	Unit
$T_{\text{unit}}(t)$	Transport unit internal temperature	°C
$T_{\text{amb}}(t)$	Ambient temperature	°C
$T_{\text{fr}}(t)$	Refrigerator temperature (active mode)	°C
$\dot{Q}_{\text{in}}(t)$	Heat inflow rate	W
R_{unit}	Thermal resistance of unit	°C/W
C_{unit}	Thermal capacity of unit	J/°C
$E_{\text{ice}}(t)$	Remaining ice energy	J
m_{ice}	Ice mass	kg
L_f	Latent heat of fusion	J/kg
T_{reset}	Reset temperature after re-icing	°C
Δt	Time step	min

Appendix B.

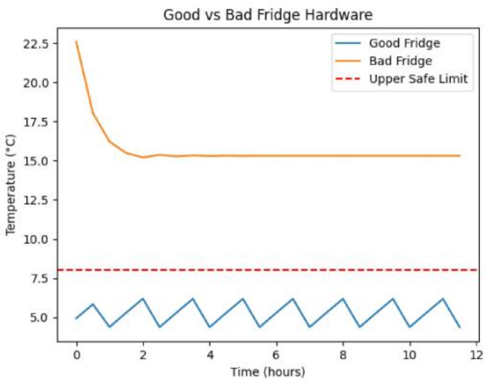

(a)

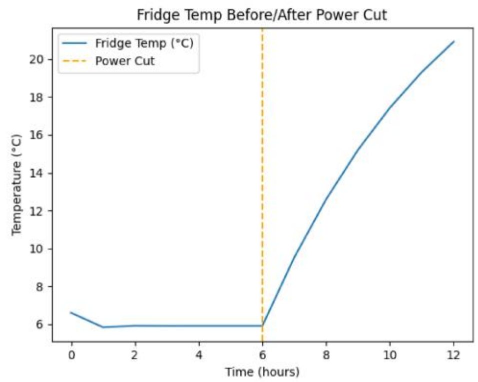

(b)

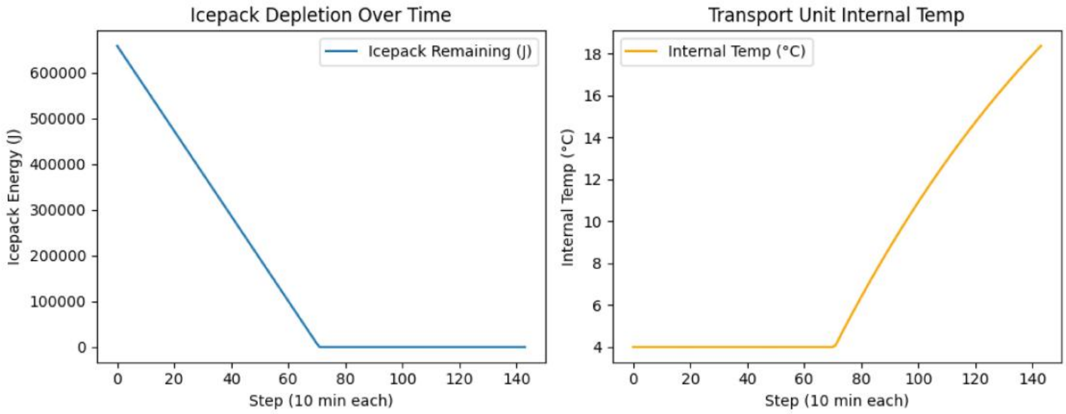

(c)

Figure B1. (a) Temperature stability in a high-insulation, high thermal mass, strong cooling ("good") vs. low-insulation, weak cooling, low thermal mass ("bad") fridge. (b) Fridge warming following a power cut after stabilization at 5.5 °C. (c) Passive transport unit using ice packs, showing stable conditions until ice depletion, after which internal temperature rises toward ambient.

Appendix C.

Table C1. Parameter modifications for Gaza conflict-affected setting interventions

Intervention	Parameter	Updated Value
Power Upgrade	Battery capacity (Wh)	8000
	Solar efficiency	0.85
	Charge efficiency	0.95
	Discharge efficiency	0.98
	Generator output (W)	4000
	Fuel capacity (L)	40
	Fuel usage (L/h)	0.7
Behavior Change	Misuse profile	Careful
	Door interval (s)	240
	Open duration (min)	1
Resilient Grid	Sabotage chance	0.002
	Grid uptime	0.9
	Blackout chance	0.0001
	Blackout hours	22–23, 8–9
	Repair delay chance	0.01
Fridge Upgrade	Fridge insulation (R-value)	6
	Clinic cooling power (W)	200
	Depot cooling power (W)	300
	Warehouse cooling power (W)	600
	Thermal mass (J/K)	10000
	Initial temperature (°C)	3

Table C2. Parameter modifications for Sudan rural conflict-affected setting interventions

Intervention	Parameter	Updated Value
Power Upgrade	Battery capacity (Wh)	10000
	Solar efficiency	0.80
	Solar panel area (m^2)	40
	Charge efficiency	0.96
	Discharge efficiency	0.97
	Generator output (W)	3000
	Fuel capacity (L)	50
	Fuel usage (L/h)	0.6
Fridge Upgrade	Fridge insulation (R-value)	6
	Clinic cooling power (W)	150
	Depot cooling power (W)	250
	Warehouse cooling power (W)	350
	Thermal mass (J/K)	8000
	Initial temperature (°C)	3
Robust Transport	Transport insulation (R-value)	3.0
	Transport delay chance	0.02
	Icepack mass (kg)	4.0
	Box volume (L)	25
	Initial temperature (°C)	3
	Looting chance	0.0005
	Roadblock chance	0.001

Table C3. Parameter modifications for Nepal highlands setting interventions

Intervention	Parameter	Updated Value
Warm Chain	Min temp override (°C)	2
	Max temp override (°C)	12
	Misuse profile	Careful
	Door interval (s)	300
	Open duration (min)	1
Route Improved	Transport delay chance	0.002
	Roadblock chance	0.002
	Looting chance	0.0005
	Repair delay chance	0.001
Container Upgrade	Transport insulation (R-value)	3.5
	Icepack mass (kg)	5.0
	Box volume (L)	30
	Initial temperature (°C)	3

Table C4. Parameter modifications for Haiti post-earthquake setting interventions

Intervention	Parameter	Updated Value
Power Hardening	Battery capacity (Wh)	8000
	Solar efficiency	0.70
	Solar peak output (W)	700
	Charge efficiency	0.97
	Discharge efficiency	0.98
	Generator output (W)	3500
	Fuel capacity (L)	60
	Fuel usage (L/h)	0.5
Mobile Units	Transport insulation (R-value)	3.2
	Box volume (L)	25
	Icepack mass (kg)	4.5
	Initial temperature (°C)	3
	Passive transport mode	Enabled
Infrastructure Shockproofing	Repair delay chance	0.01
	Grid uptime	0.6
	Blackout chance	0.25
	Sabotage chance	0.001
	Battery theft chance	0.005
Community Training	Misuse profile	Careful
	Tampering chance	0.005
	Door interval (s)	240
	Open duration (min)	1